Analysis of Shear-Thickening in Physical Gel. A Stochastic Theory for Polymer Networks

T. Indei and T. Arimitsu
Institute of Physics, University of Tsukuba, Ibaraki 305-8571, Japan
(Dated: February 1, 2008)

A formula of steady shear viscosity is derived by introducing a model to describe the dynamics of physically cross-linked network (physical gel), and successfully analyzes the shear-thickening behavior observed in HEUR aqueous solutions by Jenkins, Sileibi and El-Aasser. We take into account the effects of looped chains at junctions which detach their one end from the junction as the shear rate increases due to the collisions with other chains. This process produces the weak and wide enhancement of the number of chains whose both ends stick to the separate junctions (active chains) leading to the weak increase in the shear viscosity. It is also shown that the nonlinear force sustained by active chains induces the strong and sharp enhancement of the steady shear viscosity.

PACS numbers:
Keywords:

I. INTRODUCTION

One observes generally that the viscosity of polymer solution monotonically decreases when one increases shear rate. This effect, referred to as *shear-thinning*, results from the disentanglement of polymer chains under the shear flow. However, some sort of polymer solutions exhibit an unusual behavior, called *shear-thickening*, i.e., the viscosity of the solution grows as the shear rate increases, attains a maximum and decreases at higher shear rates.

The shear-thickening phenomenon is observed for polymers having a few segments capable of association, such as hydrophilic polymers containing a few hydrophobic groups,[1,2,3,4,5,6,7] and ionomers.[8,9] In solution, these associative polymers construct a physically cross-linked network due to temporary connections among their associative segments (physical gel). A typical example of such a physical gel is HEUR (hydrophobically modified ethoxylated urethane) aqueous solution.[1,2,3,4,5,6,7] HEUR is a hydrophilic poly(ethylene oxide) containing hydrophobic hydrocarbon groups at its both ends. In water, the hydrocarbon groups at their ends associate with each other due to hydrophobic interactions among them to construct a physically cross-linked network at relatively low polymer concentrations. Another example is a solution of telechelic ionomers in apolar solvent,[8,9] such as a solution of α,ω-Mg carboxylato-polyisoprene in decahydronaphthalene.[8]

In this paper, we study linear chains having associative functional groups at both their ends, and analyze the steady shear viscosity of HEUR aqueous solutions observed by Jenkins *et al.*[1] representing shear-thickening.[10] We will consider three types of chains in the model, i.e., *active chains* with its both ends connecting to separate junctions, *dangling chains* with only one of its end sticking to a junction and *loops* with both ends connecting to a junction (Figure 1). Floating (free) chains in solvent are not taken into account in the present approach. We introduce loops since HEUR in water has been observed to form flowerlike micelles comprised primarily of loops, as schematically depicted in Figure 1, for broad polymer concentrations above the onset of association.[3] A dangling chain can become either an active chain or a loop by connecting, respectively, its one free end to a junction with which its other end does not stick or has already stuck. In other words, an active chain can become a loop via dangling state and vice verse. We take into account the breaking of a loop by detaching its one end from a junction due to the collisions with dangling chains or other loops as the shear rate increases. It will be seen that this process produces the weak and wide enhancement of the number of active chains, leading to the weak increase in the shear viscosity. The idea of increase in the number of active chains around the shear-thickening region has been suggested from an observation that the plateau modulus there is larger than that in the Newtonian region.[6] It will be also shown that the nonlinear force of active chains described by the inverse Langevin function induces the strong and sharp enhancement of the steady shear viscosity. The effect of the nonlinear force has been discussed by others in different approaches both theoretically[11,12] and experimentally[13]. The success in the analysis of the shear viscosity in HEUR aqueous solutions by the present theoretical formula reveals that both the increase in the number of active chains and the nonlinear force of active chains are *indispensable* to understand the shear-thickening behavior.

Physical gel is a polymer network in which junctions can break and recombine due to thermal fluctuation, i.e., the junctions have the finite lifetime. The *transient network theory*, formed first by Green and Tobolsky,[14] is a powerful tool to investigate the rheological property of such gels. They extended the classical model of rubber elasticity so as to allow for the junctions which break and reform with constant rate independent of shear rate. Due to the assumptions of the constant breaking rate of junctions and of the Gaussian chains, they could not succeed to derive any non-linear rheological behavior. Lodge[15] generalized the Green-Tobolsky (GT) model by intro-

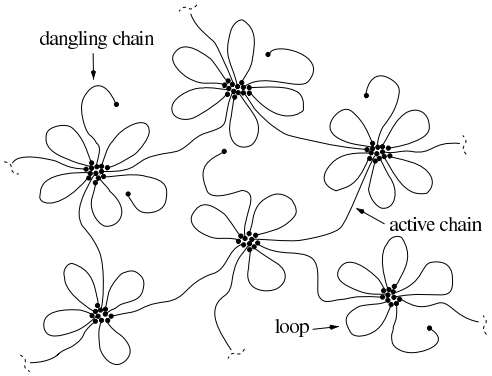

FIG. 1: Schematic representation of a network constructed by HEUR in aqueous solution.[3]

ducing the distribution in the lifetime of junctions (the inverse of breaking rate of junctions) which does not depend on the shear rate. Like the GT model, obtained shear viscosity did not depend on the shear rate, i.e., there was neither shear-thinning nor shear-thickening. On the other hand, Yamamoto[16] evolved the GT model by introducing the breakage rate of junctions which depends on the end-to-end length of a section of chain lying between two neighboring junctions (partial chain). Since the flow changes the end-to-end length of partial chains, the breakage rate must depend on the rate of flow. By assuming that the junction breaks whenever the end-to-end length of the partial chain exceeds a certain critical value under the flow and that the polymer chain is Gaussian, he showed that shear-thinning appears. This is because the number of partial chains decreases as the shear rate grows.

With the intention to analyze the physical gel comprised of linear chains having functional groups at their each end, like HEUR, Tanaka and Edwards[17,18] developed the transient network model formed by Yamamoto by introducing two types of chains in the network, i.e., the active chain and the dangling chain. Similar to the Yamamoto model, they adopted the breakage rate depending on the end-to-end length of active chains. Assuming that the breakage rate is an increasing function of the end-to-end length of an active chain without a cutoff, and that the active chain is Gaussian with linear force, they obtained the shear-thinning behavior, but could not the shear-thickening.

Wang[19] extended the Tanaka-Edwards (TE) model by introducing free chains with both ends being not connected to any junctions in addition to active and dangling chains. Like Tanaka and Edwards, he adopted the increasing breakage rate of an active chain without introducing a cutoff to its end-to-end length. He assumed that shear flow promotes creation of more free chains which collide with junctions resulting in the growth of the transition rate from a free chain to a dangling chain. Hence, the number of dangling chains grows as the shear rate increases, leading to the enhancement of the number of active chains which induces shear-thickening. However, the adoption of this transition rate appears to be somewhat doubtful, since it may not be affected by the frequency of collisions of a free chain with junctions but affected by the number of junctions surrounding the ends of free chains.[34]

All the transient network models mentioned above have one common assumption, i.e., the relaxation time of dangling (and free) chains is much smaller than that of the network. Under the assumption, a dangling chain immediately relaxes to, say, the Gaussian chain after its connected end detaches from a junction. Vaccaro and Marrucci[20] considered the network model composed of active and dangling chains, however, in order to avoid the above assumption, they introduced a 'Fokker-Planck equation' for the distribution of the end-to-end vector of dangling chains. They adopted the nonlinear Warner force[21] for active chains, and introduced the breakage rate of active chains which increases with their end-to-end length. They also introduced the recombination rate linearly increasing with respect to the end-to-end length of dangling chains. For the relaxation time τ of chains having the order of the lifetime (at equilibrium state) β_0^{-1} of active chains, shear-thickening is shown to appear. On the other hand, as seen in subsection V B, the relaxation time of chains in the experiment we are going to analyze[1] is estimated as $\tau \simeq 10^{-5} \sim 10^{-4}$s, while $\beta_0^{-1} \simeq 10^{-2} \sim 10^{-1}$s. For such short relaxation time ($\tau \ll \beta_0^{-1}$), shear-thickening does not seem to appear within their model. Therefore, we need to propose other mechanism to explain the shear-thickening phenomenon even in the case $\tau \ll \beta_0^{-1}$.

The transient network theory may be also applicable to the topologically entangled polymer system when the entanglement points are regarded as junctions since the entanglements formed by chains can be disentangled due to the thermal agitation of chains along the tube-like region comprised of surrounding chains, i.e., reptation proposed by de Gennes.[22] Actually, Yamamoto evolved his model with the intention to treat polymer solutions at rather high concentration. However, the topological restriction of chains is only effectively taken into account in this treatment. Doi and Edwards[23] developed a theory for the concentrated polymer solutions or melts on the basis of the reptation model. They succeeded, for example, to derive shear-thinning behavior for a topologically entangled system comprised of linear chains.

In the present paper, we will focus our attention on the system where the above effect of the topological entanglement is week and negligible, since in the experiment we will analyze, the polymer concentration is at most on the order of the overlap threshold of polymer chains (see subsection V A). Junctions are ascribed to the association among functional groups at each end of linear chains.

In section II, we introduce the basic equation dealing with the physically cross-linked network composed

of unentangled linear chains with associative functional groups at both their ends. The derived equation, representing the transition among each type of the chains, will be used throughout in this paper for the analysis of the steady shear viscosity of physical gel. In section III, the dynamics of each type of chains and the transition rates among them under the steady shear flow will be discussed. We see that the transition from a loop to a dangling chain is promoted by the shear flow. It plays an important role in the shear-thickening phenomena as well as the nonlinear force of active chains. In section IV, we solve the basic equation introduced in section II in order to give a formula for the steady shear viscosity. In section V, we analyze the experimentally observed shear viscosity of HEUR aqueous solutions[1] by the obtained formula. It will be shown that the formula explains experiments quite well for the broad shear rate. Discussions will be devoted to section VI.

II. BASIC EQUATION

A. Assumptions

We treat in this paper the system made up of linear chains which are uniformly distributed in space, with uniform molecular weight, carrying associative groups at both their ends. No topological entanglements are considered. Here we list again the three types of chains relevant to our model (Figure 1): 1) *Active chain*: The both ends of the chain are connected to two junctions separated in space. 2) *Dangling chain*: Only one of the two ends is connected to a junction. 3) *Loop*: Both ends are connected to a single junction.

Suppose the situation in which an incompressible macro-deformation is added to the uniform system. We assume that the distribution of chains remains uniform even after the application of the deformation. Hereafter, we will pay our attention to those phenomena taking place in an *arbitrary* unit volume in the system. The number of chains n per unite volume is constant in time thanks to the incompressibility of the deformation, and in space due to the homogeneity of the system.

The added deformation produces a velocity-field in the system causing a conformation change of chains. We represent the conformation of a chain by means of its end-to-end vector.

B. End-to-End Vector Space

Now, we introduce a space, named the *end-to-end vector space*, in which we will construct a basic equation for the end-to-end vector of chains. In this space, all chains which have the same end-to-end vector are represented by one point called a *representative point* for the chains. Since our system consists of those chains which have the same contour length, say l, all representative points locate within the sphere of radius l. Note that the representative point have nothing to do with a position of chain in real space. Even if a chain moves around in real space, its representative point does not move unless the chain changes its end-to-end vector.

Thermodynamical quantities related to a chain, such as tension, free energy and so on, are often given by functions of its end-to-end vector $\mathbf{r}$. The end-to-end vector space provides us with the support of these functions.

C. Equation for the Number of Chains

1. Eulerian Description

Let us introduce, in unit volume in real space, the number $\phi^i(\mathbf{r},t)d\mathbf{r}$ of i-chains with end-to-end vector $\mathbf{r}\sim\mathbf{r}+d\mathbf{r}$ at time t. The superscript i distinguishes the type of chains, i.e., $i=a$ represents active chains, $i=d$ dangling chains and $i=l$ loops. Note that the total number $\phi(\mathbf{r},t)d\mathbf{r}$ of chains with end-to-end vector $\mathbf{r}\sim\mathbf{r}+d\mathbf{r}$ in unit volume is given by

$$\phi(\mathbf{r},t)d\mathbf{r}=\sum_i \phi^i(\mathbf{r},t)d\mathbf{r}. \tag{2.1}$$

We derive the equation for $\phi^i(\mathbf{r},t)$ in the end-to-end vector space for i-chains under the velocity-field $\dot{\mathbf{r}}^i(\mathbf{r},t)$ caused by the deformation added to the system.

Let us consider a volume $V^i(t)$, in the end-to-end vector space for i-chains, which varies its boundary in accordance with $\dot{\mathbf{r}}^i(\mathbf{r},t)$. Since the points for i-chains in this volume are created or annihilated, we have the equation for number-conservation of i-chains

$$\frac{d}{dt}\left(\int_{V^i(t)} d\mathbf{r}\ \phi^i(\mathbf{r},t)\right) = -\sum_{j(\neq i)}\int_{V^i(t)} d\mathbf{r}\ W_{ji}(\mathbf{r},t)\phi^i(\mathbf{r},t) + \sum_{j(\neq i)}\int_{V^i(t)} d\mathbf{r}\ W_{ij}(\mathbf{r},t)\phi^j(\mathbf{r},t), \tag{2.2}$$

where $W_{ij}(\mathbf{r},t)dt$ is the transition probability during dt at time t from j-chains to i-chains having the same end-to-end vector $\mathbf{r}$ (see Figure 2). The conservation of the transition probability $W_{ij}(\mathbf{r},t)dt$ reads

$$\sum_i W_{ij}(\mathbf{r},t)dt=1. \tag{2.3}$$

The first term in the right-hand side of (2.2) represents the number of i-chains in $V^i(t)$ which convert to other types of chains in unit time, whereas the second term stands for the number of $j(\neq i)$-chains in $V^i(t)$ which convert to i-chains in unit time. That is, the first and the second terms represent annihilation and creation of i-chains, respectively. As $V^i(t)$ is arbitrary, we obtain the equation for $\phi^i(\mathbf{r},t)$ from (2.2)

$$\frac{\partial}{\partial t}\phi^i(\mathbf{r},t)+\frac{\partial}{\partial \mathbf{r}}\cdot\left(\dot{\mathbf{r}}^i(\mathbf{r},t)\phi^i(\mathbf{r},t)\right)$$

$$= -\sum_{j(\neq i)} W_{ji}(\mathbf{r})\phi^i(\mathbf{r},t) + \sum_{j(\neq i)} W_{ij}(\mathbf{r})\phi^j(\mathbf{r},t). \quad (2.4)$$

When the *total* number of chains does not change, $\phi(\mathbf{r},t)$ satisfies an equation

$$\frac{\partial}{\partial t}\phi(\mathbf{r},t) + \frac{\partial}{\partial \mathbf{r}} \cdot \left(\dot{\mathbf{r}}(\mathbf{r},t)\phi(\mathbf{r},t) \right) = 0. \quad (2.5)$$

The requirement that the summation of (2.4) with respect to i should coincide with (2.5) gives us the relation between $\dot{\mathbf{r}}(\mathbf{r},t)$ and $\dot{\mathbf{r}}^i(\mathbf{r},t)$ in the form

$$\dot{\mathbf{r}}(\mathbf{r},t)\phi(\mathbf{r},t) = \sum_i \dot{\mathbf{r}}^i(\mathbf{r},t)\phi^i(\mathbf{r},t). \quad (2.6)$$

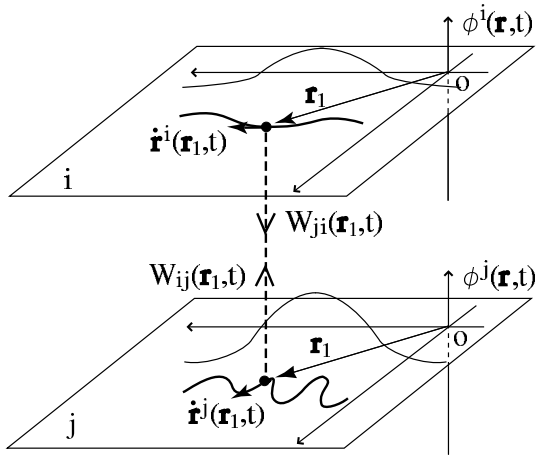

FIG. 2: Schematic explanation of transitions between i-chains and j-chains having the same end-to-end vector $\mathbf{r}_1$ at time t (Eulerian description). The upper plane (actually three dimensional) stands for the end-to-end vector space for i-chains and the lower for j-chains. A solid line in the end-to-end vector space for α-chains ($\alpha = i, j$) represents a streamline for α-chains passing through a point $\mathbf{r}_1$ at t. The streamline gives the velocity $\dot{\mathbf{r}}^\alpha(\mathbf{r},t)$ as its tangent line at $\mathbf{r}$. A representative point for α-chains moves in accordance with $\dot{\mathbf{r}}^\alpha(\mathbf{r},t)$ in each end-to-end vector space as described by (2.4).

2. *Lagrangian Description*

The basic equation (2.4) of the present paper is the one in the Eulerian description. Since, hereafter, we will analyze mainly in the Lagrangian description, we introduce the quantity

$$\phi^i(\mathbf{r}^i(t;\mathbf{r}_0^i,t_0),t) = \int d\mathbf{r}\ \delta(\mathbf{r} - \mathbf{r}^i(t;\mathbf{r}_0^i,t_0))\phi^i(\mathbf{r},t), \quad (2.7)$$

in the description where $\mathbf{r}^i(t;\mathbf{r}_0^i,t_0)$ is a position of the representative point belonging to i-chains at t, which was located at $\mathbf{r}_0^i$ at the initial time t_0. $\mathbf{r}^i(t;\mathbf{r}_0^i,t_0)$ is a solution of the equation of motion

$$\frac{d\mathbf{r}^i(t)}{dt} = \dot{\mathbf{r}}^i(\mathbf{r}^i(t),t), \quad (2.8)$$

with the initial condition $\mathbf{r}^i(t_0;\mathbf{r}_0^i,t_0) = \mathbf{r}_0^i$. The equation of motion (2.8) describes the dynamics of the end-to-end vector in real space, which corresponds to the movement of a representative point under the influence of the flow $\dot{\mathbf{r}}^i(\mathbf{r},t)$ in the end-to-end vector space.

Now, we derive the equation for $\phi^i(\mathbf{r}^i(t;\mathbf{r}_0^i,t_0),t)$. Differentiating (2.7) with respect to t, we have

$$\frac{d\phi^i(\mathbf{r}^i(t),t)}{dt} + \frac{1}{J^i(t,t_0)}\frac{dJ^i(t,t_0)}{dt}\phi^i(\mathbf{r}^i(t),t)$$
$$= \int d\mathbf{r}\ \delta(\mathbf{r} - \mathbf{r}^i(t))\left(\frac{\partial \phi^i(\mathbf{r},t)}{\partial t} + \frac{\partial}{\partial \mathbf{r}} \cdot \left(\dot{\mathbf{r}}^i(\mathbf{r},t)\phi^i(\mathbf{r},t) \right) \right), \quad (2.9)$$

where $J^i(t,t_0)$ is the Jacobian defined by

$$J^i(t,t_0) = \left| \frac{\partial r_\alpha^i(t)}{\partial r_{0\beta}^i} \right|. \quad (2.10)$$

For simplicity, we are omitting $\mathbf{r}_0^i$ and t_0 in $\mathbf{r}^i(t;\mathbf{r}_0^i,t_0)$. By putting the equation (2.4) within the Eulerian description into (2.9) and by multiplying $J^i(t,t_0)$ on both sides, (2.9) reduces to

$$\frac{d}{dt}\left(J^i(t,t_0)\phi^i(\mathbf{r}^i(t),t) \right)$$
$$= -\sum_{j(\neq i)} W_{ji}(\mathbf{r}^i(t),t)J^i(t,t_0)\phi^i(\mathbf{r}^i(t),t)$$
$$+ \sum_{j(\neq i)} W_{ij}(\mathbf{r}^i(t),t)J^i(t,t_0)\phi^j(\mathbf{r}^i(t),t). \quad (2.11)$$

A transition to the i-chain with end-to-end vector $\mathbf{r}^i(t)$ (or to the region $d\mathbf{r}^i(t) = J^i(t,t_0)d\mathbf{r}_0^i$ in the end-to-end vector for i-chains) can occur only from the j-chains ($j \neq i$) whose end-to-end vector $\mathbf{r}^j(t)$ is equal to $\mathbf{r}^i(t)$ (or from the end-to-end vector space for j-chains whose region $d\mathbf{r}^j(t) = J^j(t,t_0)d\mathbf{r}_0^j$ is equal to $d\mathbf{r}^i(t)$). Therefore, the arguments of W_{ij} and ϕ^j in the second term of the right-hand side of (2.11) are $\mathbf{r}^i(t)$ instead of $\mathbf{r}^j(t)$ (or the superscript of the Jacobian $J^i(t,t_0)$ is i instead of j) (see Figure 3).

Integrating (2.11) from time t_0 to t, we have

$$J^i(t,t_0)\phi^i(\mathbf{r}^i(t;\mathbf{r}_0^i,t_0),t)$$
$$= \exp\left[-\int_{t_0}^t dt' \sum_{j(\neq i)} W_{ji}(\mathbf{r}^i(t';\mathbf{r}_0^i,t_0),t') \right]\phi^i(\mathbf{r}_0^i,t_0)$$
$$+ \int_{t_0}^t dt' \exp\left[-\int_{t'}^t dt'' \sum_{j(\neq i)} W_{ji}(\mathbf{r}^i(t'';\mathbf{r}_0^i,t_0),t'') \right]$$

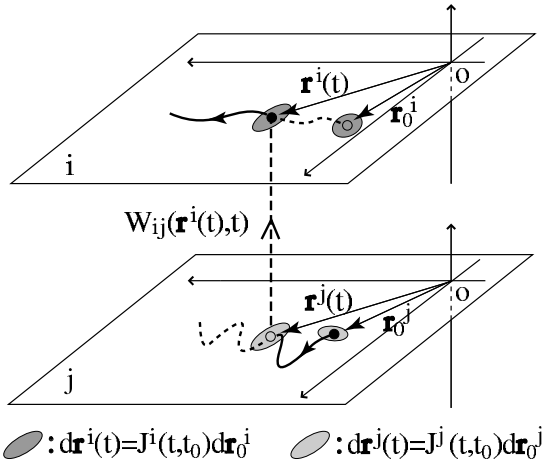

FIG. 3: Schematic explanation of the transition from j-chains to i-chains (Lagrangian description). A solid line in the end-to-end vector space for i-chains (upper plane) expresses a trajectory of a representative point for i-chains which was at $\mathbf{r}_0^i$ at time t_0. On the other hand, a solid line in the end-to-end vector space for j-chains (lower plane) represents a trajectory of a representative point for j-chains passing through a point $\mathbf{r}^j(t)$ which is equal to $\mathbf{r}^i(t)$ at the moment t. The dark-gray region at $\mathbf{r}^i(t)$ in the upper plane represents a domain $d\mathbf{r}^i(t) = J^i(t,t_0)d\mathbf{r}_0^i$ whereas the light-gray region around $\mathbf{r}^j(t)(=\mathbf{r}^i(t))$ in the lower plain is $d\mathbf{r}^j(t) = J^j(t,t_0)d\mathbf{r}_0^j$ which is equal to $d\mathbf{r}^i(t)$.

$$\times \sum_{j(\neq i)} W_{ij}(\mathbf{r}^i(t';\mathbf{r}_0^i,t_0),t')J^i(t',t_0)\phi^j(\mathbf{r}^i(t';\mathbf{r}_0^i,t_0),t'). \tag{2.12}$$

The first term in the right-hand side of (2.12) expresses the number of i-chains with end-to-end vector $\mathbf{r}^i(t) \sim \mathbf{r}^i(t)+d\mathbf{r}^i(t)$ which were i-chain having the end-to-end vector $\mathbf{r}_0^i \sim \mathbf{r}_0^i + d\mathbf{r}_0^i$ at time t_0, and remain i-chain until time t. This term vanishes at $t \to \infty$ in most cases. The second term represents the number of i-chains with $\mathbf{r}^i(t) \sim \mathbf{r}^i(t)+d\mathbf{r}^i(t)$ which became i-chain at t' ($> t_0$), and remain i-chain until time t.

D. Stochastic Process

When the dynamics of i-chains is given by a stochastic process, say $\mathbf{R}(t)$, $\dot{\mathbf{r}}^i(\mathbf{r},t)$ becomes stochastic $\dot{\mathbf{r}}^i(\mathbf{r},t;\mathbf{R}(t))$. In this case, $\phi^i(\mathbf{r},t)$ becomes also stochastic $\phi^i(\mathbf{r},t;\mathbf{R}(t))$ through (2.4). Hereafter, we denote $\dot{\mathbf{r}}^i(\mathbf{r},t;\mathbf{R}(t))$ as $\dot{\mathbf{r}}_f^i(\mathbf{r},t)$ and $\phi^i(\mathbf{r},t;\mathbf{R}(t))$ as $\phi_f^i(\mathbf{r},t)$ for simplicity. The equations for $\phi^i(\mathbf{r},t)$ in the previous subsection hold for $\phi_f^i(\mathbf{r},t)$ as well, if the products between two stochastic quantities, such as $\dot{\mathbf{r}}_f^i(\mathbf{r},t)\phi_f^i(\mathbf{r},t)$, are regarded as the Stratonovich-type products.[24] By replacing $\phi^i(\mathbf{r},t)$ and $\dot{\mathbf{r}}^i(\mathbf{r},t)$ with $\phi_f^i(\mathbf{r},t)$ and $\dot{\mathbf{r}}_f^i(\mathbf{r},t)$ respectively, (2.4) becomes

$$\frac{\partial}{\partial t}\phi_f^i(\mathbf{r},t) + \frac{\partial}{\partial \mathbf{r}}\cdot\left(\dot{\mathbf{r}}_f^i(\mathbf{r},t)\phi_f^i(\mathbf{r},t)\right) = -\sum_{j(\neq i)} W_{ji}(\mathbf{r},t)\phi_f^i(\mathbf{r},t) + \sum_{j(\neq i)} W_{ij}(\mathbf{r},t)\phi_f^j(\mathbf{r},t), \tag{2.13}$$

and by replacing $\phi^i(\mathbf{r}^i(t),t)$ and $\mathbf{r}^i(t)$ with $\phi_f^i(\mathbf{r}_f^i(t),t)$ and $\mathbf{r}_f^i(t)$ respectively, (2.12) becomes

$$\begin{aligned} &J^i(t,t_0)\phi_f^i(\mathbf{r}_f^i(t;\mathbf{r}_0^i,t_0),t) \\ &= \exp\left[-\int_{t_0}^t dt' \sum_{j(\neq i)} W_{ji}(\mathbf{r}_f^i(t';\mathbf{r}_0^i,t_0),t')\right]\phi_f^i(\mathbf{r}_0^i,t_0) \\ &+ \int_{t_0}^t dt' \exp\left[-\int_{t'}^t dt'' \sum_{j(\neq i)} W_{ji}(\mathbf{r}_f^i(t'';\mathbf{r}_0^i,t_0),t'')\right] \\ &\times \sum_{j(\neq i)} W_{ij}(\mathbf{r}_f^i(t';\mathbf{r}_0^i,t_0),t')J^i(t',t_0)\phi_f^j(\mathbf{r}_f^i(t';\mathbf{r}_0^i,t_0),t'), \end{aligned} \tag{2.14}$$

where $\mathbf{r}_f^i(t;\mathbf{r}_0^i,t_0)$ is a solution of the Langevin equation

$$\frac{d\mathbf{r}^i(t)}{dt} = \dot{\mathbf{r}}^i(\mathbf{r}^i(t),t;\mathbf{R}(t)) = \dot{\mathbf{r}}_f^i(\mathbf{r}^i(t),t), \tag{2.15}$$

with the initial condition $\mathbf{r}_f^i(t_0;\mathbf{r}_0^i,t_0) = \mathbf{r}_0^i$. An equation (2.13) corresponds to the 'stochastic Liouville equation' in the end-to-end vector space for i-chains.[25] In the following, we will denote by $\langle\langle\cdots\rangle\rangle$ the average with respect to the stochastic process.

E. Remarks

In the present model, features of each type of chains are characterized through $\dot{\mathbf{r}}_f^i(\mathbf{r},t)$ and $W_{ij}(\mathbf{r},t)$. We will give functional forms of $\dot{\mathbf{r}}_f^i(\mathbf{r},t)$ and $W_{ij}(\mathbf{r},t)$ in the next section when the system is in the incompressible velocity gradient $\hat{\kappa}(t)$, especially, in the steady shear flow.

III. CHARACTERIZATION

A. Tension in a Chain

When the distance between two ends of a flexible chain is finite, say $\mathbf{r}$, there appears an effective attractive force $\mathbf{f}(\mathbf{r})$ between these ends, due to the thermal motion of segments within the chain. We adopt, for the attractive force, the one obtained within the random-flight model:

$$\mathbf{f}(\mathbf{r}) = -\frac{k_BT}{a}L^{-1}\left(\frac{r}{Na}\right)\frac{\mathbf{r}}{r}, \tag{3.1}$$

where L^{-1} is the inverse function of the Langevin function defined by $L(x)=\coth x-1/x$. Here and hereafter, N is the number of statistical segments in a chain, a the length of a segment, T temperature of the solution in which chains are immersed and k_B the Boltzmann constant. Note that in the random-flight model, the finiteness of the contour length $l=Na$ of a chain is taken into account seriously.

B. Dynamics in End-to-End Vector Space

1. Active Chain

We assume that all junctions move in accordance with the velocity gradient $\hat{\kappa}(t)$, and that the effects of the fluctuation of junctions are week and negligible (affine deformation assumption). Since the end points $\mathbf{x}_1^a(t)$ and $\mathbf{x}_2^a(t)$ of an active chain in real space are sticking to *different* junctions by definition, the end-to-end vector $\mathbf{r}^a(t)$, defined by $\mathbf{r}^a(t)=\mathbf{x}_1^a(t)-\mathbf{x}_2^a(t)$, has finite value whose time evolution is given by

$$\frac{d\mathbf{r}^a(t)}{dt}=\hat{\kappa}(t)\mathbf{r}^a(t). \tag{3.2}$$

The equation (3.2) is equivalent to the velocity-field

$$\dot{\mathbf{r}}^a(\mathbf{r},t)=\hat{\kappa}(t)\mathbf{r} \tag{3.3}$$

in the end-to-end vector space for active chains. It means that if a representative point at $\mathbf{r}$ belongs to active chains at t, it flows in accordance with $\dot{\mathbf{r}}^a(\mathbf{r},t)$. Integrating (3.2) from time t_0 to t, we have

$$\mathbf{r}^a(t;\mathbf{r}_0^a,t_0)=\mathrm{T}\exp\left[\int_{t_0}^t dt'\hat{\kappa}(t')\right]\mathbf{r}_0^a\equiv\hat{\lambda}(t,t_0)\mathbf{r}_0^a, \tag{3.4}$$

where T is the time-ordered operator. In the case of steady flows, since $\hat{\kappa}$ is independent of time, $\hat{\lambda}(t;t')$ becomes a function of the time interval $t-t'$, i.e., $\hat{\lambda}(t;t')=\exp[(t-t')\hat{\kappa}]\equiv\hat{\lambda}(t-t')$.

2. Dangling Chain

One end of a dangling chain connects to a junction (we call it connected end), whereas the other end does not (we call it free end). We treat the free end as a Brownian particle, i.e., the free end changes its position randomly by the random force $\mathbf{R}(t)$ acting on it. Let $\mathbf{x}_1^d$ stands for the position of the free end of a dangling chain, and $\mathbf{x}_2^d$ the position of its connected end in real space. Dynamics of $\mathbf{x}_1^d$ is determined by the Langevin equation

$$\zeta_N\left(\frac{d\mathbf{x}_1^d(t)}{dt}-\hat{\kappa}(t)\mathbf{x}_1^d(t)\right)=\mathbf{f}(\mathbf{x}_1^d(t)-\mathbf{x}_2^d(t))+\mathbf{R}(t), \tag{3.5}$$

where we neglected the inertial term ($\propto d^2\mathbf{x}_1^d(t)/dt^2$) since the relaxation time for the velocity of typical polymer chains are usually much smaller than the time region of our interest.[26] ζ_N is the friction constant between a chain and a solvent, which is assumed to be $\zeta_N\simeq N\zeta_1$ where ζ_1 is the friction constant per segment. ζ_1 is given by Stokes's law: $\zeta_1=6\pi\eta_s a$ with η_s being the viscosity of the solvent. The random force $\mathbf{R}(t)$ in (3.5) is assumed to be the Gaussian white process, i.e., its average and variance are given by

$$\langle\!\langle R_\alpha(t)\rangle\!\rangle=0, \tag{3.6}$$

$$\langle\!\langle R_\alpha(t)R_\beta(s)\rangle\!\rangle=2\zeta_N k_BT\delta_{\alpha\beta}\delta(t-s), \tag{3.7}$$

respectively ($\alpha,\beta=x,y,z$). The dynamics of $\mathbf{x}_2^d$ is determined in accordance with $\hat{\kappa}(t)$:

$$\frac{d\mathbf{x}_2^d(t)}{dt}=\hat{\kappa}(t)\mathbf{x}_2^d(t). \tag{3.8}$$

Making use of (3.5) and (3.8), we obtain the equation for the time evolution of the end-to-end vector $\mathbf{r}^d(t)=\mathbf{x}_1^d(t)-\mathbf{x}_2^d(t)$ in the form

$$\frac{d\mathbf{r}^d(t)}{dt}=\hat{\kappa}(t)\mathbf{r}^d(t)+\frac{1}{\zeta_N}\left(\mathbf{f}(\mathbf{r}^d(t))+\mathbf{R}(t)\right). \tag{3.9}$$

The equation (3.9) is equivalent to the velocity-field

$$\dot{\mathbf{r}}_f^d(\mathbf{r},t)=\hat{\kappa}(t)\mathbf{r}+\frac{1}{\zeta_N}\left(\mathbf{f}(\mathbf{r})+\mathbf{R}(t)\right) \tag{3.10}$$

in the end-to-end vector space for dangling chains. It means that if a representative point at $\mathbf{r}$ belongs to dangling chains at t, it flows in accordance with $\dot{\mathbf{r}}_f^d(\mathbf{r},t)$.

When the Hookean approximation is adopted for the tension $\mathbf{f}(\mathbf{r})$, i.e.,

$$\mathbf{f}(\mathbf{r})=-K_N\mathbf{r}\ \ (\equiv\mathbf{f}_N^0(\mathbf{r})),\qquad K_N=\frac{3k_BT}{Na^2}, \tag{3.11}$$

the equation of motion (3.9) and the corresponding velocity-field (3.10) become

$$\frac{d\mathbf{r}^d(t)}{dt}=\left(\hat{\kappa}(t)-\frac{K_N}{\zeta_N}\right)\mathbf{r}^d(t)+\frac{1}{\zeta_N}\mathbf{R}(t) \tag{3.12}$$

and

$$\dot{\mathbf{r}}_f^d(\mathbf{r},t)=\left(\hat{\kappa}(t)-\frac{K_N}{\zeta_N}\right)\mathbf{r}+\frac{1}{\zeta_N}\mathbf{R}(t), \tag{3.13}$$

respectively. The equation of motion (3.12) is analytically integrated from t_0 to t as

$$\mathbf{r}_f^d(t;\mathbf{r}_0^d,t_0)=\mathrm{e}^{-(t-t_0)/2\tau}\hat{\lambda}(t,t_0)\mathbf{r}_0^d+\frac{1}{\zeta_N}\int_{t_0}^t dt'\mathrm{e}^{-(t-t')/2\tau}\hat{\lambda}(t,t')\mathbf{R}(t'), \tag{3.14}$$

where τ is the relaxation time of a dangling chain defined by

$$\tau = \frac{\zeta_N}{2K_N} \simeq \frac{\zeta_1 N^2 a^2}{6k_B T}. \tag{3.15}$$

The Hookean approximation (3.11) is valid when the end-to-end length of a dangling chain is short enough compared with its contour length. This situation is realized when the relaxation time (3.15) for the end-to-end vector of a dangling chain is much shorter than the characteristic time of the deformation.

3. Loop

The end-to-end distance of a loop is *always* zero, i.e.,

$$\mathbf{r}^l(t; \mathbf{r}_0^l = 0, t_0) = 0, \qquad (\text{for any } t(> t_0)). \tag{3.16}$$

The equation (3.16) is equivalent to the velocity-field

$$\dot{\mathbf{r}}^l(\mathbf{r} = 0, t) = 0, \qquad (\text{for any } t). \tag{3.17}$$

in the end-to-end vector space for loops. It means that if a representative point at $\mathbf{r} = 0$ belongs to loops at t, it does not flow. Note that no information about the conformation of a chain is obtained from (3.16) or (3.17).

Now, we estimate the dimension of a loop in a steady shear flow. Let $\mathbf{x}(n,t)$ be a position of the nth segment ($n = 1, \cdots, N$) of a chain in real space at time t. The Langevin equation for segments is written, for $n = 2, \cdots, N-1$, as

$$\begin{aligned}
&\zeta_1 \left(\frac{d\mathbf{x}(n,t)}{dt} - \hat{\kappa}(t)\mathbf{x}(n,t) \right) \\
&= \mathbf{f}_1^0(\mathbf{x}(n,t) - \mathbf{x}(n+1,t)) + \mathbf{f}_1^0(\mathbf{x}(n,t) - \mathbf{x}(n-1,t)) \\
&\quad + \mathbf{R}(n,t) \qquad (3.18) \\
&= K_1 \frac{\partial^2 \mathbf{x}(n,t)}{\partial n^2} + \mathbf{R}(n,t) \qquad (3.19)
\end{aligned}$$

where, in (3.18), we substituted (3.11) for the force $\mathbf{f}_{N=1}^0$ between neighboring two segments along the chain, and took the continuous limit for n. The random force $\mathbf{R}(n,t)$, acting on the segment at $\mathbf{x}(n,t)$, is assumed to be the Gaussian white process, i.e., its average and variance are given by

$$\langle\langle R_\alpha(n,t) \rangle\rangle = 0, \tag{3.20}$$

$$\langle\langle R_\alpha(n,t) R_\beta(m,s) \rangle\rangle = 2\zeta_1 k_B T \delta_{\alpha\beta} \delta(n-m) \delta(t-s), \tag{3.21}$$

respectively. Since one end of a loop connects with its another end, the boundary condition at $n = 0$ and $N = 0$ should be

$$\mathbf{x}(n=0,t) = \mathbf{x}(n=N,t) = 0, \tag{3.22}$$

where we fixed the connected point at the origin without loss of generality. The property of a loop is characterized through (3.22).

Making use of (3.19) with (3.22), we can get the *mean-square radius of gyration* $s_\alpha s_\beta$ of a loop defined by

$$\begin{aligned}
&s_\alpha s_\beta \\
&= \frac{1}{N} \int_0^N dn \langle\langle [x_\alpha(n,t) - x_{G\alpha}(n,t)][x_\beta(n,t) - x_{G\beta}(n,t)] \rangle\rangle
\end{aligned} \tag{3.23}$$

under a deformation. Here, $\mathbf{x}_G(t) = N^{-1} \int_0^N dn \mathbf{x}(n,t)$ is the center of mass of a loop. When a steady shear deformation with shear rate $\dot{\gamma}$, described by the deformation tensor

$$\hat{\lambda}(t,t') = \begin{pmatrix} 1 & \dot{\gamma}(t-t') & 0 \\ 0 & 1 & 0 \\ 0 & 0 & 1 \end{pmatrix} \tag{3.24}$$

or the velocity gradient tensor

$$\hat{\kappa} = \begin{pmatrix} 0 & \dot{\gamma} & 0 \\ 0 & 0 & 0 \\ 0 & 0 & 0 \end{pmatrix} \tag{3.25}$$

is added, (3.23) become (see appendix A)

$$s_x^2 = \frac{Na^2}{36} \left(1 + \frac{13\pi^4}{10080} (\dot{\gamma}\tau_1)^2 \right), \tag{3.26}$$

$$s_y^2 = s_z^2 = \frac{Na^2}{36}, \tag{3.27}$$

$$s_x s_y = \frac{Na^2}{72}, \quad s_x s_z = s_y s_z = 0. \tag{3.28}$$

τ_1 is the relaxation time of a loop given by

$$\tau_1 = \frac{\zeta_1 N^2 a^2}{3\pi^2 k_B T}, \tag{3.29}$$

which is essentially equivalent to τ defined by (3.15).

C. Transition Probabilities

The j-chain becomes the i-chain with the probability W_{ij} during unit time. We suppose that the transition rates W_{ij} are affected by how many times the j-chain collides with other chains within its lifetime under the influence of a flow. Since, in most cases, the frequency of the collision depends on the velocity gradient $\hat{\kappa}(t)$ of a flow, W_{ij} is a function of t through $\hat{\kappa}(t)$ as well as the end-to-end vector $\mathbf{r}$ of the j-chain. However, at steady states in steady flows, W_{ij} becomes a function of a quantity characterizing the flow, e.g., the shear rate $\dot{\gamma}$ for the steady shear flow. In this subsection, for the shear flow given by (3.25), we introduce the dependence of W_{ij} on $\dot{\gamma}$ and $\mathbf{r}$.

In the following, for simplicity, we denote the transition W_{da} from an active to a dangling chain by β, W_{ad} from a dangling to an active chain by p, W_{ld} from a dangling

chain to a loop by v and W_{dl} from a loop to a dangling chain by u. We can put $W_{la}=W_{al}=0$ between an active chain and a loop, since the primitive transitions should occur between the dangling and other states as stated in section I.

1. Transition between Active and Dangling Chains

a. From Active to Dangling Chains An active chain becomes a dangling chain with the transition rate β by detaching its one end from a junction. In our model, β depends scarcely on $\dot\gamma$. The reason is as follows. *All* active chains alter their end-to-end vector *affinely*, therefore, they hardly collide with each other. As for the dangling chain (or the loop), since it sticks to a certain junction, its center of mass moves in accordance with $\hat\kappa$. That is, on a certain xz-plane (i.e., the plane on which the shear flow has the same velocity), the relative velocity between the active chain and the dangling chain (or the loop) is very slow. This is the reason why the frequency of the collision between the active chain and the dangling chain (or the loop) is small.

We assume that the one end of an active chain dissociates from the network definitely when its end-to-end distance becomes longer than $r^*(<Na)$. We further assume that the breakage rate $\beta(\mathbf{r})$ for $r\le r^*$ is constant and has value β_0. The breakage rate $\beta(\mathbf{r})$ under these assumptions can be written in the form[16]

$$\beta(\mathbf{r})=\begin{cases}\beta_0 & (r\le r^*)\\ \infty & (r>r^*)\end{cases}. \tag{3.30}$$

b. From Dangling to Active Chains A dangling chain becomes an active chain with the transition rate p by attaching its free end to a certain junction with which its other end of the chain does not connect. Although the dangling chain collides with other dangling chains and loops, there seems to be no reason for the collision to affect the *connecting* process of the free end to the junction. Therefore, we assume that p is independent of $\dot\gamma$. As for the $\mathbf{r}$ dependence, we can regard p as a constant effectively, since the connecting process does not seem to be affected strongly by the end-to-end vector.

2. Transition between Dangling Chains and Loops

a. From Dangling Chains to Loops A dangling chain becomes a loop with the transition rate v by attaching its free end to the junction with which its other end has already stuck. Since the connecting process is not influenced by the collision with other chains as stated above, $v(\vec r)$ can be assumed to be independent of $\dot\gamma$.

Since the process takes place only when its end-to-end length is 0, we can write $v(\mathbf{r})$ as

$$v(\mathbf{r})=v_0\delta(\mathbf{r})V, \tag{3.31}$$

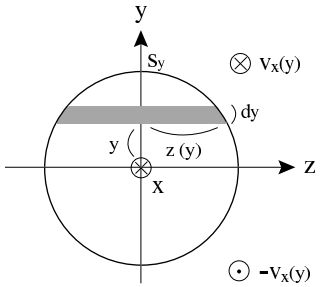

FIG. 4: Schematic picture of a region occupied by a loop, represented as a sphere with a radius of s_y. Monomers in the region $y>0$ enter into this domain along the x-axis, whereas segments in $y<0$ along the $-x$ direction.

where V is the quantity having the dimension of the volume (see (4.17)).

b. From Loops to Dangling Chains A loop becomes a dangling chain with the transition rate u by detaching its one end from the junction with which its both ends has stuck. The *disconnecting* process of the loop are influenced by collisions with dangling chains and other loops.

Since the transitions from the *active* chain to the dangling chain is also the disconnecting process of one end from a junction, the breakage rate $u(\dot\gamma)$ for the loop when $\dot\gamma=0$ should be the same as the detaching rate for the *active* chain appeared in (3.30), i.e., $u(\dot\gamma=0)=\beta_0$. Let us introduce the quantity $u(\dot\gamma)/\beta_0$ $(\dot\gamma\neq0)$ which stands for the probability for the loop to dissociate during the time duration $1/\beta_0$. Note that $1/\beta_0$ stands for the lifetime of loops when $\dot\gamma=0$. The ratio $u(\dot\gamma)/\beta_0$ must be larger than 1, since the collisions of other chains with the backbone of the loop affects the possibility for its one of the ends to disconnect from the junction. We can assume that the increment A of $u(\dot\gamma)/\beta_0$, defined by

$$A=\frac{u(\dot\gamma)}{\beta_0}-1, \tag{3.32}$$

is given by the number of *segments* colliding with the loop *during its lifetime*. The collisions take place when the segments enter into the region occupied by the loop. We assume that the radius of the region is given by its radius of gyration.

Under the above assumption, A is estimated as follows. Let the center of mass of a loop be the origin. Denoting by s_y the radius of gyration of the loop of y-component (see (3.27)), the number of segments $\nu_{in}^{d,l}(y)dy$ belonging to dangling chains and loops, which enter into a region $y\sim y+dy$ $(y>0)$ and $-z(y)\sim z(y)$ occupied by the loop (see Figure 4) in unit time, is given by

$$\begin{aligned}\nu_{in}^{d,l}(y)dy&=(\nu^d+\nu^l)N\cdot 2z(y)\ dy\cdot v_x(y)\\&=2(\nu^d+\nu^l)N\sqrt{(s_y)^2-y^2}\ \dot\gamma y\ dy,\end{aligned} \tag{3.33}$$

where we used $z(y)=\sqrt{(s_y)^2-y^2}$ and $v_x(y)=\dot\gamma y$. ν^i $(i=d,l)$ is the number of i-chains per unit volume.

Integrating (3.33) from 0 to s_y and multiplying by 2 to take account of the region $y<0$, we have the number of segments entering into the domain occupied by the loop in unit time:

$$2\int_0^{s_y} dy\ \nu_{in}^{d,l}(y) = (\nu^d+\nu^l)N\frac{4}{3}(s_y)^3\dot\gamma = \frac{4}{3\cdot 36^{3/2}}(\nu^d+\nu^l)a^3N^{5/2}\dot\gamma, \quad (3.34)$$

where we substituted s_y given by (3.27) for the second equality. Dividing (3.34) by $u(\dot\gamma)$, we obtain

$$A = \frac{1}{162}(\nu^d+\nu^l)a^3N^{5/2}\frac{\dot\gamma}{u(\dot\gamma)}. \quad (3.35)$$

Putting (3.35) into (3.32), and solving it for $u(\dot\gamma)$, we finally get

$$u(\dot\gamma)/\beta_0 = \frac{1+\sqrt{1+\frac{1}{162}(\Phi^d+\Phi^l)N^{3/2}\dot\gamma/\beta_0}}{2}, \quad (3.36)$$

where $\Phi^i \equiv N\nu^i a^3$ is the volume fraction of i-chains. In the experiments we are going to analyze, Φ^a is much smaller than Φ^d and Φ^l, as will be shown later. In this case, $\Phi^d+\Phi^\ell$ in (3.36) can be replaced by the volume fraction Φ of all chains. Note that there is no $\mathbf{r}$ dependence in $u(\dot\gamma)$, since the end-to-end length of the loop is zero.

IV. OBSERVABLE QUANTITIES

A. Zero-Shear Viscosity

Here, we derive the zero-shear viscosity η_0. Since we treat the case in which the shear rate $\dot\gamma$ is much smaller than β_0, $\beta(r)$ can be regarded as β_0. We use the basic equations (2.13) written in terms of the Eulerian description. Substituting (3.3), (3.13) and (3.17) into (2.13), we have a set of equations for $\phi_f^a(\mathbf{r},t)$, $\phi_f^d(\mathbf{r},t)$ and $\phi_f^l(\mathbf{r},t)$:

$$\frac{\partial}{\partial t}\phi_f^a(\mathbf{r},t) + \nabla\cdot\left(\left[\hat\kappa(t)\mathbf{r}\right]\phi_f^a(\mathbf{r},t)\right) = -\beta_0\phi_f^a(\mathbf{r},t) + p\phi_f^d(\mathbf{r},t), \quad (4.1)$$

$$\frac{\partial}{\partial t}\phi_f^d(\mathbf{r},t) + \nabla\cdot\left(\left[\left(\hat\kappa(t)-\frac{K_N}{\zeta_N}\right)\mathbf{r}+\frac{1}{\zeta_N}\mathbf{R}(t)\right]\phi_f^d(\mathbf{r},t)\right) = \beta_0\phi_f^a(\mathbf{r},t) - (p+v(\mathbf{r}))\phi_f^d(\mathbf{r},t) + u\phi_f^l(\mathbf{r},t), \quad (4.2)$$

$$\frac{\partial}{\partial t}\phi_f^l(\mathbf{r},t) = v(\mathbf{r})\phi_f^d(\mathbf{r},t) - u\phi_f^l(\mathbf{r},t). \quad (4.3)$$

Taking average with respect to the stochastic process $\mathbf{R}(t)$ in above equations, we obtain

$$\frac{\partial}{\partial t}\phi^a(\mathbf{r},t) + \nabla\cdot\left(\left[\hat\kappa(t)\mathbf{r}\right]\phi^a(\mathbf{r},t)\right) = -\beta_0\phi^a(\mathbf{r},t) + p\phi^d(\mathbf{r},t), \quad (4.4)$$

$$\frac{\partial}{\partial t}\phi^d(\mathbf{r},t) + \nabla\cdot\left(\left[\left(\hat\kappa(t)-\frac{K_N}{\zeta_N}\right)\mathbf{r}-\frac{k_BT}{\zeta_N}\nabla\right]\phi^d(\mathbf{r},t)\right) = \beta_0\phi^a(\mathbf{r},t) - (p+v(\mathbf{r}))\phi^d(\mathbf{r},t) + u\phi^l(\mathbf{r},t), \quad (4.5)$$

$$\frac{\partial}{\partial t}\phi^l(\mathbf{r},t) = v(\mathbf{r})\phi^d(\mathbf{r},t) - u\phi^l(\mathbf{r},t). \quad (4.6)$$

We will give their derivations in appendix B. The equation (4.2) corresponds to the *stochastic Liouville equation*,[25] whereas the equation (4.5) is equivalent to the *Fokker-Planck equation*.[35]

In the long time limit $t\to\infty$, $\phi^i(\mathbf{r},t)$ becomes independent of time (we denote it as $\phi^i(\mathbf{r})$). Letting $\frac{\partial}{\partial t}\phi^i(\mathbf{r},t)=0$ $(i=a,d,l)$ in the above equations, we have

$$\nabla\cdot\left(\hat\kappa\mathbf{r}\phi^a(\mathbf{r})\right) = -\beta_0\phi^a(\mathbf{r}) + p\phi^d(\mathbf{r}), \quad (4.7)$$

$$\nabla\cdot\left(\left[\left(\hat\kappa-\frac{K_N}{\zeta_N}\right)\mathbf{r}-\frac{k_BT}{\zeta_N}\nabla\right]\phi^d(\mathbf{r})\right) = \beta_0\phi^a(\mathbf{r}) - (p+v(\mathbf{r}))\phi^d(\mathbf{r}) + u\phi^l(\mathbf{r}), \quad (4.8)$$

$$v(\mathbf{r})\phi^d(\mathbf{r}) = u\phi^l(\mathbf{r}). \quad (4.9)$$

With the help of (4.9), we can eliminate $\phi^l(\mathbf{r})$ in (4.8):[36]

$$\nabla\cdot\left(\left[\left(\hat\kappa-\frac{K_N}{\zeta_N}\right)\mathbf{r}-\frac{k_BT}{\zeta_N}\nabla\right]\phi^d(\mathbf{r})\right) = \beta_0\phi^a(\mathbf{r}) - p\phi^d(\mathbf{r}). \quad (4.10)$$

1. Number of Chains in the Absence of Flow

The number of i-chains per unit volume in real space is given by

$$\nu^i = \int d\mathbf{r}\ \phi^i(\mathbf{r}). \quad (4.11)$$

According to (2.1), we obtain the equation for the number-conservation

$$n = \nu^a + \nu^d + \nu^l, \quad (4.12)$$

where n is the total number of chains in unit volume:

$$n = \int d\mathbf{r}\ \phi(\mathbf{r}). \quad (4.13)$$

In the current situation of the slow shear flow, ν^i is expanded in powers of $\dot\gamma$: $\nu^i = \nu_0^i + \nu_1^i|\dot\gamma| + \cdots$. Since the zeroth order term ν_0^i contributes to η_0 as seen later, we now derive the expression for ν_0^i, i.e., the number of i-chains in unit volume at the equilibrium state. Integrating (4.7) or (4.10) for $\hat\kappa=0$, we have

$$0 = -\beta_0\nu_0^a + p\nu_0^d. \quad (4.14)$$

Integrating (4.9) for $\hat{\kappa}=0$, we obtain

$$v_0 V \phi_0^d(\mathbf{r}=0) = \beta_0 \nu_0^l, \tag{4.15}$$

where $\phi_0^i(\mathbf{r})$ means $\phi^i(\mathbf{r})$ at the equilibrium state, and we put $u=\beta_0$ since $\dot{\gamma}=0$. Let us now introduce $\psi(\mathbf{r})$ by

$$\phi_0^d(\mathbf{r}) = \nu_0^d \psi(\mathbf{r}). \tag{4.16}$$

Note that because of (4.11), $\psi(\mathbf{r})$ is normalized as $\int d\mathbf{r}\psi(\mathbf{r})=1$. Defining V by

$$V = \frac{1}{\psi(\mathbf{r}=0)}, \tag{4.17}$$

(4.15) reduces to

$$v_0 \nu_0^d = \beta_0 \nu_0^l. \tag{4.18}$$

Solving (4.14) and (4.18) with the help of (4.12), we obtain

$$\nu_0^a = \frac{n}{1+\frac{\beta_0}{p}(1+\frac{v_0}{\beta_0})}, \tag{4.19}$$

$$\nu_0^d = \frac{n}{1+\frac{p}{\beta_0}+\frac{v_0}{\beta_0}}, \tag{4.20}$$

$$\nu_0^l = \frac{n}{1+\frac{\beta_0}{v_0}(1+\frac{p}{\beta_0})}. \tag{4.21}$$

2. Root-Mean-Square of End-to-End Vector

Hereafter, we denote the expectation value of the physical quantity $A(\mathbf{r})$ with respect to the i-chain as

$$\langle A(\mathbf{r})\rangle^i = \frac{\int d\mathbf{r} A(\mathbf{r})\phi^i(\mathbf{r})}{\int d\mathbf{r}\phi^i(\mathbf{r})} = \frac{1}{\nu^i}\int d\mathbf{r} A(\mathbf{r})\phi^i(\mathbf{r}). \tag{4.22}$$

Multiplying the equation (4.7) and (4.10) by $r_\alpha r_\beta$, and integrating them with respect to $\mathbf{r}$, we have

$$-\kappa_{\alpha\gamma}\langle r_\gamma r_\beta\rangle^a \nu^a - \langle r_\alpha r_\gamma\rangle^a \kappa_{\beta\gamma}\nu^a = -\beta_0\langle r_\alpha r_\beta\rangle^a\nu^a + p\langle r_\alpha r_\beta\rangle^d\nu^d, \tag{4.23}$$

$$-\kappa_{\alpha\gamma}\langle r_\gamma r_\beta\rangle^d\nu^d - \langle r_\alpha r_\gamma\kappa_{\beta\gamma}\rangle^d\nu^d + \frac{2K_N}{\zeta_N}\langle r_\alpha r_\beta\rangle^d\nu^d - \frac{2k_BT}{\zeta_N}\delta_{\alpha\beta}\nu^d = \beta_0\langle r_\alpha r_\beta\rangle^a\nu^a - p\langle r_\alpha r_\beta\rangle^d\nu^d. \tag{4.24}$$

Substituting (3.25) for $\hat{\kappa}$, we obtain

$$-2\dot{\gamma}\langle xy\rangle^a\nu^a = -\beta_0\langle x^2\rangle^a\nu^a + p\langle x^2\rangle^d\nu^d, \tag{4.25}$$

$$-\dot{\gamma}\langle y^2\rangle^a\nu^a = -\beta_0\langle xy\rangle^a\nu^a + p\langle xy\rangle^d\nu^d, \tag{4.26}$$

$$0 = -\beta_0\langle y^2\rangle^a\nu^a + p\langle y^2\rangle^d\nu^d, \tag{4.27}$$

$$-\frac{2k_BT}{\zeta_N}\nu^d + \frac{2K_N}{\zeta_N}\langle xy\rangle^d\nu^d - 2\dot{\gamma}\langle xy\rangle^d\nu^d = \beta_0\langle x^2\rangle^a\nu^a - p\langle x^2\rangle^d\nu^d, \tag{4.28}$$

$$\frac{2K_N}{\zeta_N}\langle xy\rangle^d\nu^d - \dot{\gamma}\langle y^2\rangle^d\nu^d = \beta_0\langle xy\rangle^a\nu^a - p\langle xy\rangle^d\nu^d, \tag{4.29}$$

$$-\frac{2k_BT}{\zeta_N} + \frac{2K_N}{\zeta_N}\langle y^2\rangle^d\nu^d = \beta_0\langle y^2\rangle^a\nu^a - p\langle y^2\rangle^d\nu^d, \tag{4.30}$$

where we put $x=r_1$, $y=r_2$ and $z=r_3$. Solving the above equations, we get root-mean-square of the end-to-end vector for the active and the dangling chain in the form

$$\langle x^2\rangle^a = \frac{Na^2}{3}\left[1+2\left(\frac{\dot{\gamma}}{\beta_0}\right)^2 + 2(\dot{\gamma}\tau)^2\left\{\left(1+\frac{p}{\beta_0}\right)^2 + \frac{1}{\beta_0\tau}\left(1+\frac{2p}{\beta_0}\right)^2\right\}\right], \tag{4.31}$$

$$\langle xy\rangle^a = \frac{Na^2}{3}\left[\frac{\dot{\gamma}}{\beta_0} + \dot{\gamma}\tau\left(1+\frac{p}{\beta_0}\right)\right], \tag{4.32}$$

$$\langle y^2\rangle^a = \frac{Na^2}{3}, \tag{4.33}$$

$$\langle x^2\rangle^d = \frac{Na^2}{3}\left[1+2(\dot{\gamma}\tau)^2\left\{\left(1+\frac{p}{\beta_0}\right)^2 + \frac{p}{\beta_0^2\tau}\right\}\right], \tag{4.34}$$

$$\langle xy\rangle^d = \frac{Na^2}{3}\dot{\gamma}\tau\left(1+\frac{p}{\beta_0}\right), \tag{4.35}$$

$$\langle y^2\rangle^d = \frac{Na^2}{3}, \tag{4.36}$$

$$\left(\langle z^2\rangle^a = \langle z^2\rangle^d = \frac{Na^2}{3}, \quad (\text{others})=0\right) \tag{4.37}$$

where τ is given by (3.15).

3. Zero-Shear Viscosity

The shear stress caused by i-chains is given by

$$\sigma_{xy}^i = \nu^i\langle\frac{xy}{r}f(r)\rangle^i. \tag{4.38}$$

We can use the linear form for the tension $f(r)$ of the chain, since, when $\dot{\gamma} \ll \beta_0$, the end-to-end length r of the chain stays sufficiently short during the deformation compared with its contour length. Putting $f(r)=K_N r$ into (4.38), we have

$$\sigma_{xy}^i = K_N\nu^i\langle xy\rangle^i. \tag{4.39}$$

With the help of (4.32), we obtain the shear stress caused by active chains in the form

$$\sigma_{xy}^a = k_BT\nu^a\left[\frac{\dot{\gamma}}{\beta_0} + \dot{\gamma}\tau\left(1+\frac{p}{\beta_0}\right)\right] = k_BT\nu_0^a\left[\frac{\dot{\gamma}}{\beta_0} + \dot{\gamma}\tau\left(1+\frac{p}{\beta_0}\right)\right] + O(\dot{\gamma}^2), \tag{4.40}$$

where ν_0^a is given by (4.19). Then, the zero-shear viscosity is obtained as

$$\eta_0^a = \lim_{\dot{\gamma}\to 0}\frac{\sigma_{xy}^a}{\dot{\gamma}} = k_BT\nu_0^a\left[\frac{1}{\beta_0} + \tau\left(1+\frac{p}{\beta_0}\right)\right]. \tag{4.41}$$

Similarly, with the help of (4.35), the shear stress caused by dangling chains becomes

$$\sigma_{xy}^d = k_B T \nu_0^d \dot{\gamma}\tau\left(1+\frac{p}{\beta_0}\right)+O(\dot{\gamma}^2), \qquad (4.42)$$

where ν_0^d is given by (4.20), and the zero-shear viscosity is obtained as

$$\eta_0^d = \lim_{\dot{\gamma}\to 0}\frac{\sigma_{xy}^d}{\dot{\gamma}} = k_B T \nu_0^d \tau\left(1+\frac{p}{\beta_0}\right). \qquad (4.43)$$

The total zero-shear viscosity is given by $\eta_0 = \eta_0^a + \eta_0^d$.

4. Remarks on the Relaxation Time

In the experiments we are going to analyze,[1] the relaxation time τ ($\simeq 10^{-5}$s, see the next section for its estimation) given by (3.15) is always much shorter than the specific time $1/\dot{\gamma}(=10^{-3}\sim 10^{-1}$s) of the shear flow. In this case, as we can see from (4.40) and (4.42), the effect of τ becomes very week for $\dot{\gamma}$ smaller than $1/\tau(\simeq 10^5$s). Consequently, we will adopt the limit $\tau\to 0$ from now on. In this limit, the dangling chain has always stress-free conformation which is regarded as the Gaussian.[37] Then $\phi^d(\mathbf{r})$ is written, even for finite $\dot{\gamma}$ (see (4.16)), as

$$\phi^d(\mathbf{r}) = \nu^d \psi(\mathbf{r}), \qquad (4.44)$$

where

$$\psi(\mathbf{r}) = \left(\frac{3}{2\pi N a^2}\right)^{3/2}\exp\left[-\frac{3r^2}{2Na^2}\right]. \qquad (4.45)$$

The total zero-shear viscosity becomes at $\tau\to 0$

$$\eta_0 = \nu_0^a \frac{k_B T}{\beta_0} = \frac{n}{1+\frac{\beta_0}{p}(1+\frac{v_0}{\beta_0})}\frac{k_B T}{\beta_0}. \qquad (4.46)$$

B. Non-Newtonian Viscosity

Here, we investigate the shear viscosity for the shear rate including larger than $1/\beta_0$. To this end, we analyze the basic equations (2.12) written in terms of the Lagrangian description,[38] since this description connects $\phi^a(\mathbf{r},t)$ (and $\phi^l(\mathbf{r},t)$) with $\psi(\mathbf{r})$.

1. Equation for Active Chains

The equation for the active chains is given by putting $i=a$ in (2.12) as

$$\begin{aligned} &J^a(t,t_0)\phi^a(\mathbf{r}^a(t;\mathbf{r}_0,t_0),t) \\ &= \exp\left[-\int_{t_0}^t dt'\ \beta(\mathbf{r}^a(t';\mathbf{r}_0,t_0))\right]\phi^a(\mathbf{r}_0,t_0) \\ &\quad + p\int_{t_0}^t dt'\ \exp\left[-\int_{t'}^t dt''\beta(\mathbf{r}^a(t'';\mathbf{r}_0,t_0))\right] \\ &\qquad \times J^a(t',t_0)\nu^d(t')\psi(\mathbf{r}^a(t';\mathbf{r}_0,t_0)), \end{aligned} \qquad (4.47)$$

where we used the relation

$$\phi^d(\mathbf{r},t) = \nu^d(t)\psi(\mathbf{r}). \qquad (4.48)$$

$\psi(\mathbf{r})$ is given by (4.45). Recall that $\mathbf{r}^a(t;\mathbf{r}_0,t_0)$ in (4.47) is given by (3.4). In order to obtain the equation for the expectation value of $A(\mathbf{r})$ with respect to the active chain, let us multiply the equation (4.47) by $A(\mathbf{r}^a(t;\mathbf{r}_0,t_0))$ and integrate it with respect to $\mathbf{r}_0$:

$$\begin{aligned} &\int d\mathbf{r}\ A(\mathbf{r})\phi^a(\mathbf{r},t) \\ &= \int d\mathbf{r}\exp\left[-\int_{t_0}^t dt'\beta(\mathbf{r}^a(t';\mathbf{r},t_0))\right]A(\mathbf{r}^a(t;\mathbf{r},t_0))\phi^a(\mathbf{r},t_0) \\ &\quad + p\int_{t_0}^t dt'\int d\mathbf{r}\exp\left[-\int_{t'}^t dt''\beta(\mathbf{r}^a(t'';\mathbf{r},t'))\right] \\ &\qquad \times A(\mathbf{r}^a(t;\mathbf{r},t'))\nu^d(t')\psi(\mathbf{r}). \end{aligned} \qquad (4.49)$$

In deriving (4.49), we changed the integration variable from $\mathbf{r}^a(t;\mathbf{r}_0,t_0)$ to $\mathbf{r}$ in the left-hand side of (4.49), and from $\mathbf{r}^a(t';\mathbf{r}_0,t_0)$ to $\mathbf{r}$ in the second term of the right-hand side. Under the steady flow, due to $\lambda(t;t') = \lambda(t-t')$, (4.49) reduces to

$$\begin{aligned} &\int d\mathbf{r}\ A(\mathbf{r})\phi^a(\mathbf{r},t) \\ &= \int d\mathbf{r}\exp\left[-\int_0^{t-t_0} dt'\beta(\mathbf{r}^a(t';\mathbf{r}))\right]A(\mathbf{r}^a(t-t_0;\mathbf{r}))\phi^a(\mathbf{r},t_0) \\ &\quad + p\int_0^{t-t_0} dt'\int d\mathbf{r}\exp\left[-\int_0^{t'} dt''\beta(\mathbf{r}^a(t'';\mathbf{r}))\right] \\ &\qquad \times A(\mathbf{r}^a(t';\mathbf{r}))\nu^d(t-t')\psi(\mathbf{r}), \\ &= \int_{D'_{r^*}(t-t_0)} d\mathbf{r}\ \mathrm{e}^{-\beta_0(t-t_0)}A(\mathbf{r}^a(t-t_0;\mathbf{r}))\phi^a(\mathbf{r},t_0) \\ &\quad + p\int_0^{t-t_0} dt'\int_{D'_{r^*}(t')} d\mathbf{r}\ \mathrm{e}^{-\beta_0 t'}A(\mathbf{r}^a(t';\mathbf{r}))\nu^d(t-t')\psi(\mathbf{r}), \end{aligned} \qquad (4.50)$$

where

$$\mathbf{r}^a(t;\mathbf{r}) = \hat{\lambda}(t)\mathbf{r} \qquad (4.51)$$

and

$$D'_{r^*}(t) = \{\mathbf{r}\mid r^a(t';\mathbf{r})\le r^*\ (\forall t'\le t)\}. \qquad (4.52)$$

A steady state can be obtained by taking the limit $t\to\infty$ and $t_0\to-\infty$. Clearly, the first term in the right-hand side of (4.50) becomes 0 in these limit. As for the second term, because of $t\to\infty$, $\nu^d(t-t')$ can be regarded as the value ν^d in the steady state for $t'<\infty$. On the other hand, for $t'\to\infty$, the integrand becomes

exponentially small due to the factor $\mathrm{e}^{-\beta_0 t'}$. Therefore, $\nu^d(t-t')$ is always regarded as ν^d in the limit of steady state. Hence, (4.22) for $i=a$ becomes

$$\langle A(\mathbf{r})\rangle^a = p\frac{\nu^d}{\nu^a}\int_0^\infty dt \int_{D'_{r^*}(t)} d\mathbf{r}\ \mathrm{e}^{-\beta_0 t} A(\mathbf{r}^a(t;\mathbf{r}))\psi(\mathbf{r}). \quad (4.53)$$

Hereafter, we will take

$$D_{r^*}(t) = \{\mathbf{r} \mid r^a(t;\mathbf{r}) \le r^*\} \quad (4.54)$$

instead of $D'_{r^*}(t)$ as the region of the integration in (4.53) as far as the steady shear flow is concerned. Then the contribution to the integration (4.53) from the region outside $D'_{r^*}(t)$ (i.e., $r=r^a(t=0;\mathbf{r})>r^*$) emerges. Recall that the Gaussian distribution function $\psi(\mathbf{r})$ in the integrand of (4.53) mainly weighs the contribution from r smaller than $\sqrt{N}a$. Since it turns out that r^* is close to Na, the contribution from the region $r > r^*(\simeq Na \gg \sqrt{N}a)$ is almost negligible. Therefore, we can substitute safely the region $D_{r^*}(t)$ for $D'_{r^*}(t)$.

2. Equation for Loops

The equation for the loops is written as

$$\begin{aligned} J^l(t,t_0)\phi^l(\mathbf{r}^l(t;t_0,\mathbf{r}_0),t) &= \mathrm{e}^{-u(t-t_0)}\phi^l_f(\mathbf{r}_0,t_0) \\ &+ \int_{t_0}^t dt' \mathrm{e}^{-u(t-t')} J^l(t',t_0)\nu^d(t') \\ &\times v(\mathbf{r}^l(t';t_0,\mathbf{r}_0))\psi(\mathbf{r}^l(t';t_0,\mathbf{r}_0),t'). \end{aligned} \quad (4.55)$$

Following the same procedure as the case of active chains, we have the equation for the expectation value of $A(\mathbf{r})$ with respect to the loop:

$$\begin{aligned} \int d\mathbf{r} A(\mathbf{r})\phi^l(\mathbf{r}) &= \frac{\nu^d}{\nu^l}\int_0^\infty dt \int d\mathbf{r}\ \mathrm{e}^{-ut} v(\mathbf{r}) A(\mathbf{r}^l(t;\mathbf{r}))\psi(\mathbf{r}) \\ &= \frac{\nu^d}{\nu^l}\frac{v_0}{u} V\psi(0)A(0) \\ &= \frac{\nu^d}{\nu^l}\frac{v_0}{u}A(0), \end{aligned} \quad (4.56)$$

where we used V given by (4.17).

3. Number of Chains

Putting $A(\mathbf{r}) = 1$ in (4.53), we have

$$\nu^a = p\nu^d \int_0^\infty dt \int_{D_{r^*}(t)} d\mathbf{r}\ \mathrm{e}^{-\beta_0 t}\psi(\mathbf{r}) = \nu^d \frac{p}{\zeta}, \quad (4.57)$$

where we introduced

$$\frac{1}{\zeta} = \int_0^\infty dt \int_{D_{r^*}(t)} d\mathbf{r}\ \mathrm{e}^{-\beta_0 t}\psi(\mathbf{r}). \quad (4.58)$$

Note that when $\dot\gamma \to 0$, we find $\zeta \to \beta_0$. Similarly, by putting $A(\mathbf{r})=1$ in (4.56), we have

$$\nu^l = \nu^d \frac{v_0}{u}. \quad (4.59)$$

By solving (4.58) and (4.59) with the help of (4.12), the numbers of chains per volume for each type becomes

$$\nu^a = \frac{n}{1+\frac{\zeta}{p}(1+\frac{v_0}{u})}, \quad (4.60)$$

$$\nu^d = \frac{n}{1+\frac{p}{\zeta}+\frac{v_0}{u}}, \quad (4.61)$$

$$\nu^l = \frac{n}{1+\frac{u}{v_0}(1+\frac{p}{\zeta})}. \quad (4.62)$$

4. Shear Viscosity

The shear stress caused by active chains is

$$\begin{aligned} \sigma^a_{xy} &= \nu^a \langle \frac{xy}{r} f(r)\rangle^a \\ &= p\nu^d \frac{k_B T}{a}\int_0^\infty dt \int_{D_{r^*}(t)} d\mathbf{r}\ \mathrm{e}^{-\beta_0 t} \\ &\times \frac{x^a(t;\mathbf{r})y^a(t;\mathbf{r})}{r^a(t;\mathbf{r})} L^{-1}(r^a(t;\mathbf{r}))\psi(\mathbf{r}), \end{aligned} \quad (4.63)$$

where ν^d is given by (4.61) and $\mathbf{r}^a(t,\mathbf{r})$ is given by (4.51). Recalling that the shear stress caused by dangling chains is zero, we finally get the formula of the total shear viscosity in the form

$$\eta = \frac{\sigma^a_{xy}}{\dot\gamma}. \quad (4.64)$$

C. Tanaka-Edwards Limit

Tanaka and Edwards[18] calculated the steady shear viscosity for the physical gel, composed of active and dangling chains (loops are absent), with the assumptions that 1) the breakage rate is given by $\beta(r)=\beta_0+\beta_1 r^2$ (β_0 and β_1 are constant), and 2) even the active chains can be described by Gaussian chain model with the Hookean force $f^0_N(r)=K_N r$. The assumption 1) indicates that there are finite populations of active chains nearly equal to and/or even longer than the contour length l, i.e., there is no cutoff length r^* ($< l$) in the TE model. The Gaussian chain model, proposed in the assumption 2), means that there are only shorter active chains ($r \ll l$) satisfying the Hookean force assumption. In this sense, the above two assumptions contradict each other.

This conflict between the two assumptions 1) and 2) can be resolved by introducing the cutoff length r^* much smaller than l. However, in general, there seems no reason to restrict the force to be linear. That is the reason why we adopt the force (3.1) given by the random-flight

model with the cutoff r^* $(0<r^*<l)$. Hereafter, we call the case where $r^* \ll l$ and $v_0 \to 0$ the *TE limit* within our model, since, in this case, the Hookean force is valid and loops are absent ($\nu^l = 0$).

V. ANALYSES OF EXPERIMENTS

Now, we analyze, with the help of the formulae (4.64) and (4.63) derived theoretically in this paper, the steady shear viscosity observed experimentally by Jenkins *et al.*[1] for HEUR having hexadecyl end groups in water.

A. Determination of N, a and Φ

The contour length l of HEUR is obtained if we know the fully extended length l_0 of ethylene oxide (EO), the main component of HEUR, and the number n_{rep} of EO units in HEUR, i.e., $l = l_0 \times n_{rep}$. Taking the value 1.54Å for a carbon-carbon bond length, 1.43Å for a carbon-oxygen bond length, and 70.5° for the angle formed by two bonds (tetrahedral bonds) in polymer backbone, we have $l_0 = (1.54 + 2 \times 1.43) \times \cos(70.5°/2) = 3.6$Å. Letting $M_0 (= 44)$ stands for the molecular weight of the EO unit, we have $n_{rep} = M_n/M_0$, where M_n is the molecular weight of HEUR. The values of l are listed in the third column of Table I for each M_n of the experiment.[1]

Knowing the values of the root-mean-square $\sqrt{\langle r^2 \rangle_0}$ of the end-to-end length[39] in addition to l, we can obtain the number N of segments per chain and the length a of each segment by the relations $N = l^2/\langle r^2 \rangle_0$ and $a = l/N$. Here, $\langle \cdots \rangle_0$ indicates the average taken in equilibrium state without any flow. The values of N and a are listed respectively in the fifth and sixth column of Table I. We see that the length a of the segment is almost independent of molecular weight M_n (or N). Since the fully extended length l_0 of the EO unit is 3.6Å, we can conclude that one segment contains $3 \sim 4$ units.

The volume fraction of polymers is defined by $\Phi = Nna^3$ with n being the number density of polymers. Since the number density is related to the mass density ρ of polymers by $n = \rho N_A/M_n$, the volume fraction reduces to $\Phi = 10^4 c N_A N a^3/M_n$ where N_A is the Avogadro constant. Note that the mass density ρ is related to the polymer concentration c expressed by the weight percentage by $\rho = 10^4 \times c$ (g/m^3). For each M_n, the volume fraction Φ of the $c = 1$wt% HEUR aqueous solution is listed in Table I. They are almost the same as they should be. We adopt the mean value $\Phi = 8.0 \times 10^{-2}$ of them in the following. Note that the overlap threshold of polymers, estimated as $\Phi^* \simeq Na^3/\langle r^2 \rangle_0^{3/2} \simeq N^{-1/2}$, is roughly 7×10^{-2} when $N = 227$, for instance. It indicates that the volume fraction of polymers in this system, $\Phi = 8.0 \times 10^{-2}$, is on the order of the overlap threshold.

B. Estimate of the Relaxation Time

We mentioned in the preceding section that the relaxation time τ given by (3.15) (or τ_1 given by (3.29)) is much smaller than the specific time of the flow. This is quantitatively shown for HEUR by putting the values of a and N listed in Table I into (3.29) with $T = 298$K and $\eta_s = 0.89 \times 10^{-3}$Pa·s (the viscosity of pure water at 298K, 1atm). The obtained relaxation time for each molecular weight is shown in Table II. Note that they have the order of 10^{-5}s. On the other hand, as seen from Figure 10, the interesting phenomena occur at a characteristic time in the range $10^{-3} \sim 10^{-1}$s. This is the quantitative reason why we took the limit τ (or τ_1) $\to 0$ in the previous section.

C. Adjustable Parameters

In our model, the shear viscosity η is given by (4.64) with (4.63). We see that there are four parameters in (4.63), i.e., β_0, p, v_0 and r^* (u is represented by β_0). Making use of the zero-shear viscosity obtained from the experiments.[1] we can eliminate one of three parameters β_0, p, v_0 through the relation (4.46). For instance, p is represented by β_0 and v_0 as

$$p = \frac{\beta_0 + v_0}{nk_BT/\eta_0\beta_0 - 1}, \tag{5.1}$$

or, written in terms of β_0 and v_0/p as

$$p = \frac{\beta_0}{nk_BT/\eta_0\beta_0 - 1 - (v_0/p)}. \tag{5.2}$$

Hereafter, we adopt β_0 and v_0/p (and r^*) as adjustable parameters. The ratio v_0/p is a measure representing which channels of the transitions are favorable, i.e., one is to the active, and the other to the loop from the dangling chain.

D. Shear Viscosity

In order to clarify the problems to be resolved, let us see the difference between the viscosity obtained from the TE limit (see Figure 10 in appendix C) and the experimentally observed one by subtracting the former from the latter for each molecular weight, and by translating along the abscissa so that its position of the (first) peak coincides with others. As can be seen in Figure 5, there appear two peaks. The set of peaks at lower shear rates ((i), in Figure 5) reflects the shear-thickening behavior. The height of the peaks becomes low with increasing M_n. It seems that each peak consists of two elements, i.e., one is high and narrow with strong M_n-dependence, whereas the other is low and broad with weak M_n-dependence. In the set of peaks at higher shear rates, i.e., at shear-thinning region ((ii), in Figure 5), the height of the peaks

M_n	n_{rep} $=M_n/M_0$	l (Å) $=l_0 n_{rep}$	$\sqrt{\langle r^2\rangle_0}$ (Å)	N $=l^2/\langle r^2\rangle_0$	a(Å) $=l/N$	Φ $=10^4 cN_A N a^3/M_n$
34,200	777	2,800	186	227	12.3	7.4×10^{-2}
51,000	1,160	4,180	231	327	12.8	8.1×10^{-2}
67,600	1,540	5,540	265	437	12.7	8.0×10^{-2}
84,300	1,920	6,910	301	527	13.1	8.5×10^{-2}

TABLE I: Properties of HEUR in water. M_n: number-average molecular weight,[1,27] n_{rep}: number of the EO units, l: contour length, $\sqrt{\langle r^2\rangle_0}$: root-mean-square of the end-to-end length,[27] N: number of segments, a: length of each segment and Φ: volume fraction for $c=1$wt% solution (mean value$=8.0\times10^{-2}$). $N_A=6.02\times10^{-23}$ is the Avogadro constant. For EO, $M_0=44$ and $l_0=3.6$Å.

M_n	τ_1(s)
34,200	1.3×10^{-5}
51,000	3.1×10^{-5}
67,600	5.4×10^{-5}
84,300	8.6×10^{-5}

TABLE II: Rouse relaxation time of HEUR obtained from (3.29)

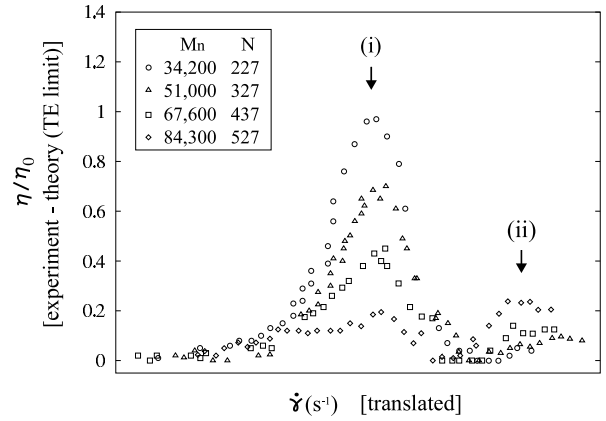

FIG. 5: The difference between theoretically (TE limit) and experimentally obtained shear viscosity. The theoretical results (lines in Figure 10 in appendix C) are subtracted from experimental data (dots in Figure 10) for each molecular weight M_n (N). To clarify the M_n dependence of the height of peaks, each data is translated so that the positions of the first peaks (i) coincide with each other.

has opposite M_n dependence compared to the previous set of peaks. We will study mainly in this paper the first peak in the following.

Let us here estimate r^* from the viewpoint of bonding energy among hydrocarbon end groups. We consider the potential barrier with height W around a junction.[18] An active chain dissociates from the junction when its one end climbs over the potential barrier W by the force $\mathbf{f}(\mathbf{r})$. Since the effective range of the hydrophobic interaction, σ, is sufficiently shorter than r^*, we can put $\sigma=a$. Then, the cut-off length r^* is roughly estimated by the condition

$$W=\int_{r'=r^*}^{r'=r^*-a} d\mathbf{r}'\cdot\mathbf{f}(\mathbf{r}')\simeq f(r^*)a. \tag{5.3}$$

The right-hand side of (5.3) represents the work done by the tension $\mathbf{f}(\mathbf{r})$ to detach the end from the junction when $r=r^*$. Assuming that $r^*\lesssim l$, we have from (3.1) $W/k_BT\simeq(1-r^*/l)^{-1}$, therefore, $r^*/l\simeq1-k_BT/W$. According to Annable *et al.*,[2] $W=28k_BT$ ($T=298$K) for HEUR of $M_w\simeq35,000$ having hexadecyl end groups (called C16/35 in the literature). In this case, r^* is estimated as $r^*\simeq0.96l$.

1. *Effects of Loops*

The number of each type of chains are plotted in Figure 6 for $r^*=0.97l$, $\beta_0=8\text{s}^{-1}$ and $v_0/p=245$ ($N=227$). With increasing the shear rate, the number ν^l of loops decreases and the number ν^d of dangling chains increases, since the transition probability u from a loop to a dangling chain increases with shear rate (see (3.36)). Due to the constant transition rate p from a dangling to an active chain, the number ν^a of active chains also increases with the same rate as the dangling chains at lower shear rates. That contributes to the gradual enhancement of the viscosity at lower shear rates as shown below. The enhancement of the number of active chains at the shear-thickening region has been observed by Tam *et al.*.[6] For higher shear rates, the population of active chains whose end-to-end length reaches r^* becomes large, which causes the decrease in ν^a leading to the shear-thinning. The numbers of active and dangling chains and the number of loops in these figures indicate that the assumption $\nu^a\ll n^d$ and $\nu^a\ll n^l$ in (3.36) is reasonable (it also holds for other values of N).

The steady shear viscosity for $r^*=0.97l$, $\beta_0=8\text{s}^{-1}$ and $v_0/p=245$ ($N=227$) is shown in Figure 7. We see that the calculated viscosity coincides well with experimental data for the broad shear rate. Note that the value $r^*=0.97l$ is quite close to the value $0.96l$ derived from the consideration based on the potential barrier between a junction and a hydrocarbon end group. In the figure,

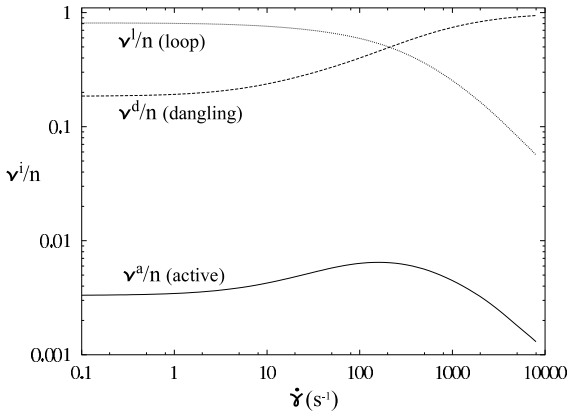

FIG. 6: The number of active chains, dangling chains and loops plotted against the shear rate for $r^*/l = 0.97$, $\beta_0 = 8\text{s}^{-1}$ and $v_0/p = 245$ ($N = 227$) corresponding to Figure 7.

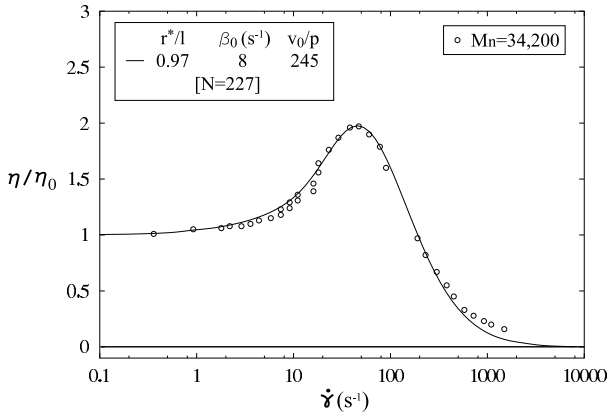

FIG. 7: The steady shear viscosity plotted against the shear rate for $N = 227$ ($M_n = 34,200$). The solid line represents the theoretical result, whereas the dots represent the experimental results observed for $\eta_0 = 3.0$Poise, $T = 298$K and $c = 1$wt%.[1]

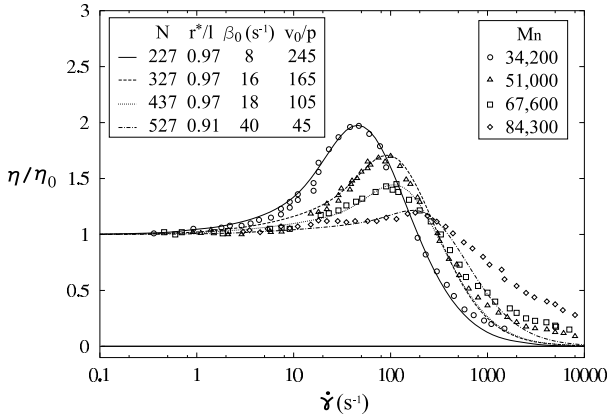

FIG. 8: The steady shear viscosity plotted against the shear rate. The lines represent theoretical results obtained for each M_n listed in Table I. The dots represent the experimental results observed for $T = 298$K and $c = 1$wt%.[1] The zero-shear viscosity η_0 is 3.0Poise for $M_n = 34,200$, 0.94Poise for $M_n = 51,000$, 0.53Poise for $M_n = 67,600$ and 0.26Poise for $M_n = 84,300$.[1]

we see the gradual enhancement of the viscosity at lower shear rates. This is because the number of active chains increases with shear rate in this region as shown in Figure 6. In addition, there is the effect of stretched active chains. It adds the sharp enhancement in the viscosity at the shear rate where the end-to-end length of the active chain reaches r^*. When loops are absent, we had to adopt r^* very close to l (see appendix C).[28] However, in the present case, since the increase in the number of active chains at lower shear rates promotes the viscosity rising, we can adopt proper value for r^*.

One might suppose that the observed shear viscosity can be fit without considering the high extension of active chains. However, it is impossible. When $r^* = 0.5l$, for instance, we cannot heighten the peak, up to the height of observed one with keeping the relation (5.1) or (5.2). Therefore, in the system we are dealing with, the above two mechanisms (i.e., the enhancement of the number of active chains and the high-extension of active chains) are indispensable.

The steady shear viscosity are calculated as shown in Figure 8 with optimal values of r^*, β_0 and v_0/p (given inside the box in the figure) for each molecular weight listed in Table I. We see from the figure that the theoretical curve for each molecular weight M_n fits very well with the first peak (although when $M_n = 84,300$, it does not fit well at higher shear rate). Note that r^* does not depend on N, except for $N = 527$.

For each v_0/p, the values of p and v_0 are given via (5.2), e.g., $p = 0.14\text{s}^{-1}$, $v_0 = 35\text{s}^{-1}$ for $v_0/p = 245$ ($N = 227$), $p = 0.1\text{s}^{-1}$, $v_0 = 17\text{s}^{-1}$ for $v_0/p = 165$ ($N = 327$) and $p = 0.065\text{s}^{-1}$, $v_0 = 6.8\text{s}^{-1}$ for $v_0/p = 105$ ($N = 437$). Assuming that p and v_0 obey, respectively, the scaling low with respect to N, i.e., $p \propto N^{-\epsilon}$ and $v_0 \propto N^{-\zeta}$, we see from these data that $\epsilon \simeq 1.2$ and $\zeta \simeq 2.5$ by the method of least squares. The dependence of p on N may be interpreted as follows. Since the polymer concentration is fixed, the number of hydrophobic end groups within the system decreases as the molecular weight increases. It diminishes the chance for a dangling chain to become an active chain. For example, when the molecular weight is doubled, the number of end groups within the system is reduced by half. This suggests $p \propto N^{-1}$ giving $\epsilon = 1$, hence the value of the exponent $\epsilon \simeq 1.2$, obtained by the present analysis, is fairly reasonable. The dependence of v_0 on N is also fairly reasonable since the probability for a self-avoiding chain to form a loop is proportional to N^{-2} giving $\zeta = 2$.[29] Recall, however, that we used just three data to determine the exponents. Obviously, we need more data in order to discuss further details of the N dependence of p and v_0. It is desirable that some

experiments will be conducted to provide enough number of data for different molecular weights which may support a more precise analysis on the N dependence.

VI. SUMMARY AND DISCUSSION

We developed the network model for physical gel composed of unentangled linear chains with associative functional groups at both their ends. The presence of three types of chains was assumed in the network system: active chains with both their ends attached to the network responsible for the stress of the system, dangling chains with one of their two ends sticking to the network and loops with both their ends connecting to a junction. We investigated the transition rates between these chains how they depend on the end-to-end vector $\mathbf{r}$ and on the shear rate $\dot{\gamma}$. The introduction of cutoff length r^* was shown to be essential for the treatment of stretched active chains. It was also revealed that the transition from a loop to a dangling chain is promoted by the shear flow because of the collision with dangling chains or other loops.

On the basis of the above network model, we showed that the origin of shear-thickening behavior is ascribed to 1) the dissociation of loops enhanced by shear flow, and 2) the high extension of active chains promoted by the flow. The portion of low and broad peak with weak N-dependence originates from the mechanism 1), and the portion of high and narrow peak with strong N-dependence stems from the mechanism 2).

It is revealed that the first peak in Figure 5 can be well explained by these two mechanisms. In Figure 9, we put the difference between theoretically obtained shear viscosity (Figure 8) and the observed shear viscosity. The disappearance of the first peak in the difference declares that we succeeded to explain the shear-thickening phenomenon by the present theoretical analysis.

In our analysis, we took the limit $\tau \to 0$ for the relaxation time of dangling chains, since the characteristic time of the shear flow is around $10^{-3} \sim 10^{-1}$s, while τ is estimated as $10^{-5} \sim 10^{-4}$s (see Table II). Within the limit $\tau \to 0$, an active chain which detaches its one end from the network relaxes to the Gaussian chains[40] in an instant, and never rejoins to the network during the relaxation. If the finite relaxation time are taken into account, on the contrary, the detached chain has the possibility to recombine with the network before it totally relaxes to the Gaussian chain.[12,20] Note that τ is larger for larger N (see (3.15)), implying that the detached chain with larger N has higher possibility to recombine with the other junction during its relaxation. It indicates that the chains with larger molecular weight contribute more to the viscosity around the shear rate where characteristic time of the flow is the same extent as that of dangling chains. We suppose that this mechanism may explain the second peak (denoted by (ii) in Figure 5 and Figure 9), since it appears at higher shear rates ($\dot{\gamma} \gtrsim 10^3 \mathrm{s}^{-1}$), and

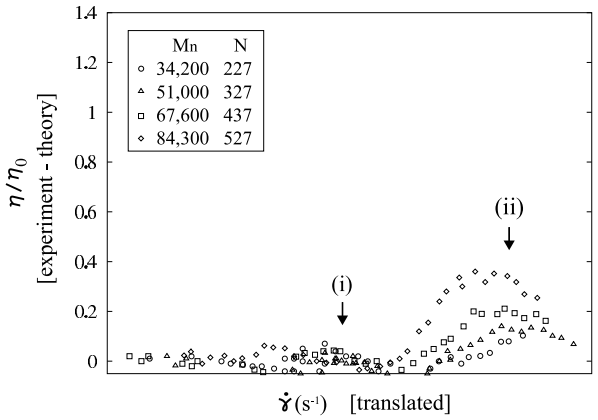

FIG. 9: The difference between experimentally and theoretically obtained shear viscosity. The theoretical results (Figure 8) are subtracted from experimental data. To clarify the N dependence of the height of peaks, each data is translated so that the positions of the observed peaks coincide with each other. See also Figure 5 for a reference.

the larger the molecular weight is, the taller the height of the peaks becomes. To include these mechanisms into the present formula is one of the interesting future problems and will be reported elsewhere.

Finally, let us comment on the idea of 'shear-induced transfer of intramolecular to intermolecular associations', proposed and investigated by Witten and Cohen[30] in qualitative ways, and developed by Ballard *et al.* in quantitative manners.[41] They considered solutions of associative polymers having some functional groups along chains. When a flow is not added to the solution, each chain is in the random coil state, and hence, has a number of associations among functional groups *inside* the chain (intramolecular associations). On the other hand, when sufficiently large velocity gradient is added to the solution, the chain extends due to viscous interactions with the solvent, thereby breaking there intramolecular associations. This causes associations among functional groups belonging to *different* chains (intermolecular associations), and enhances the viscosity. If the number of functional groups is two, and these functional groups are attached at each end of a chain, the intramolecular association makes a loop. In this case, shear-thickening is caused by 'shear-induced transfer of loops to active chains via dangling chains' in their interpretation.

One might say that this process is the same as the process proposed in the present paper. However, the origin to open a loop is quite different, i.e., as shown in section III, the dissociation of a loop is caused by collisions with other chains, in the present model. Indeed, viscous interactions with solvent affect the conformation of loops (see (3.26)), and enhance the possibility for a loop to be a dangling chain, however, this works effectively only at higher shear rates ($\dot{\gamma} \gtrsim 1/\tau_1 \sim 10^4 \mathrm{s}^{-1}$). Therefore, it seems that the dissociation of loops caused by viscous interactions

do not contribute to the shear-thickening behavior at the moderate shear rates, although they may influence the second peak in Figure 9. To include the mechanism[42] into our model is also interesting future problems.

APPENDIX A: RADIUS OF GYRATION OF A LOOP

We use the sine transform for $\mathbf{x}(n,t)$ so as to satisfy the boundary condition (3.22), i.e.,

$$\mathbf{x}(n,t) = 2\sum_{p=1}^{\infty} \mathbf{x}_p(t) \sin\left(\frac{n\pi}{N}p\right). \tag{A1}$$

We also use the sine transform for $\mathbf{R}(n,t)$, i.e.,

$$\mathbf{R}(n,t) = 2\sum_{p=1}^{\infty} \mathbf{R}_p(t) \sin\left(\frac{n\pi}{N}p\right). \tag{A2}$$

Due to (3.20) and (3.21), the average and the variance of $\mathbf{R}_p(t)$ are given by

$$\langle\!\langle R_{p\alpha}(t)\rangle\!\rangle = 0, \tag{A3}$$

$$\langle\!\langle R_{p\alpha}(t)R_{q\beta}(s)\rangle\!\rangle = \frac{\zeta_1 k_B T}{N}\delta_{\alpha\beta}\delta_{pq}\delta(t-s), \tag{A4}$$

respectively. Substituting (A1) and (A2) into (3.19), we obtain equations for $\mathbf{x}_p(t)$ as follows:

$$\frac{d\mathbf{x}_p(t)}{dt} = \left(\hat{\kappa}(t) - \frac{1}{\tau_p}\right)\mathbf{x}_p(t) + \frac{1}{\zeta_1}\mathbf{R}_p(t), \tag{A5}$$

where we put relaxation time of 'mode' p as

$$\tau_p = \frac{\zeta_1 N^2}{K_1 \pi^2}\frac{1}{p^2} = \frac{\zeta_1 N^2 a^2}{3\pi^2 k_B T}\frac{1}{p^2}. \tag{A6}$$

Integrating (A5), from time $-\infty$ to t, we have

$$\mathbf{x}_p(t) = \frac{1}{\zeta_1}\int_{-\infty}^{t} dt'\ \mathrm{e}^{-(t-t')/\tau_p}\hat{\lambda}(t,t')\mathbf{R}_p(t'). \tag{A7}$$

Making use of (A4), the correlation functions of $x_{p\alpha}(t)$ are written as

$$\langle\!\langle x_{p\alpha}(t_1)x_{q\beta}(t_2)\rangle\!\rangle = \delta_{pq}\frac{k_B T}{\zeta_1 N}\int_{-\infty}^{\min(t_1,t_2)} dt' \mathrm{e}^{-(t_1+t_2-2t')/\tau_p} \times \sum_{\gamma=1}^{3}\lambda_{\alpha\gamma}(t_1,t')\lambda_{\beta\gamma}(t_2,t'). \tag{A8}$$

For the steady shear flow represented by the deformation tensor (3.24), we have

$$\langle\!\langle x_{px}(t_1)x_{qx}(t_2)\rangle\!\rangle = \delta_{pq}\frac{Na^2}{6\pi^2}\frac{1}{p^2}\mathrm{e}^{-|t_1-t_2|/\tau_p} \times\left(1+\frac{1}{2}\tau_p\dot{\gamma}^2|t-s| + \frac{1}{2}(\tau_p\dot{\gamma})^2\right), \tag{A9}$$

$$\langle\!\langle x_{py}(t_1)x_{qy}(t_2)\rangle\!\rangle = \langle\!\langle x_{pz}(t_1)x_{qz}(t_2)\rangle\!\rangle = \delta_{pq}\frac{Na^2}{6\pi^2}\frac{1}{p^2}\mathrm{e}^{-|t_1-t_2|/\tau_p}, \tag{A10}$$

$$\langle\!\langle x_{px}(t_1)x_{qy}(t_2)\rangle\!\rangle = \delta_{pq}\frac{Na^2}{6\pi^2}\frac{1}{p^2}\mathrm{e}^{-|t_1-t_2|/\tau_p} \times\dot{\gamma}\left((t_1-t_2)\theta(t_1-t_2) + \frac{\tau_p}{2}\right), \tag{A11}$$

$$\langle\!\langle x_{px}(t_1)x_{qz}(t_2)\rangle\!\rangle = \langle\!\langle x_{py}(t_1)x_{qz}(t_2)\rangle\!\rangle = 0. \tag{A12}$$

Putting

$$\mathbf{x}_G(t) = \frac{1}{N}\int_0^N dn\ \mathbf{x}(n,t) = \frac{4}{\pi}\sum_{p:\text{odd integer}}^{\infty}\frac{\mathbf{x}_p(t)}{p} \tag{A13}$$

into (3.23), we get

$$s_\alpha s_\beta = 2\sum_{p=1}^{\infty}\langle\!\langle x_{p\alpha}(t)x_{p\beta}(t)\rangle\!\rangle - \frac{16}{\pi^2}\sum_{p,q:\text{odd integer}}^{\infty}\frac{\langle\!\langle x_{p\alpha}(t)x_{q\beta}(t)\rangle\!\rangle}{pq}. \tag{A14}$$

Substituting (A9) $\sim$ (A12) into (A14), we obtain (3.26) $\sim$ (3.28).

APPENDIX B: DERIVATION OF THE FOKKER-PLANCK EQUATION

Since $\phi_f^i(\mathbf{r},t)$ is a stochastic variable, its differentiation with respect to time is not well-defined. So, we should replace the equations (4.1) $\sim$ (4.3) by the forms of stochastic differential equations. As for (4.2), we have

$$d\phi_f^d(\mathbf{r},t) = d\Omega(\mathbf{r},t)\circ\phi_f^d(\mathbf{r},t) + \Psi_f(\mathbf{r},t)dt, \tag{B1}$$

where $\Omega(\mathbf{r},t)dt$ is the *stochastic operator* defined by

$$d\Omega(\mathbf{r},t) = -\nabla\cdot\left[\left(\hat{\kappa}(t) - \frac{K_N}{\zeta_N}\right)\mathbf{r}dt + \frac{1}{\zeta_N}d\mathbf{w}(t)\right], \tag{B2}$$

and

$$\Psi_f(\mathbf{r},t) = \beta_0\phi_f^a(\mathbf{r},t) - (p+v(\mathbf{r}))\phi_f^d(\mathbf{r},t) + u\phi_f^l(\mathbf{r},t). \tag{B3}$$

$\mathbf{w}(t)$ in (B2) is called the *Wiener process*. The correlations of its increment $d\mathbf{w}(t)$ are given by

$$\langle\!\langle dw_\alpha(t)\rangle\!\rangle = 0, \tag{B4}$$

$$\langle\!\langle dw_\alpha(t)dw_\beta(s)\rangle\!\rangle = 2\zeta_N k_B T\delta_{\alpha\beta}\delta(t-s)dtds. \tag{B5}$$

Note that the Wiener process $\mathbf{w}(t)$ is related with the Gaussian white process $\mathbf{R}(t)$ through

$$\mathbf{w}(t) = \int_0^t dt'\ \mathbf{R}(t'). \tag{B6}$$

Using the fact

$$dw_\alpha(t)dw_\beta(t)=2\zeta_N k_BT\delta_{\alpha\beta}dt, \tag{B7}$$

we obtain

$$\begin{aligned} d\Omega(\mathbf{r},t)d\Omega(\mathbf{r},t) &= \sum_{\alpha,\beta}\nabla_\alpha\nabla_\beta\frac{1}{\zeta_N^2}dw_\alpha(t)dw_\beta(t) \\ &= \nabla^2\frac{2k_BT}{\zeta_N}dt, \end{aligned} \tag{B8}$$

where we neglected the terms of order higher than dt for the first equality. Note that the product rule (B7) holds in the sense of *stochastic convergence*.[32] The relation (B8) is the content of the *fluctuation-dissipation theorem of the second kind*. Hereafter, we will omit the argument $\mathbf{r}$ in $\phi_f^d(\mathbf{r},t)$, $\Psi_f(\mathbf{r},t)$ and $\Omega(\mathbf{r},t)$ for simplicity.

In (B1), there appears the product of two stochastic variables, i.e., $\phi_f^d(t)$ and $d\mathbf{w}(t)$. There are two types of such product: one is the product of the *Ito* type[33] which is defined by

$$\phi_f^d(t)\cdot d\mathbf{w}(t)=\phi_f^d(t)[\mathbf{w}(t+dt)-\mathbf{w}(t)], \tag{B9}$$

and the other is that of the *Stratonovich* type[24] defined by

$$\phi_f^d(t)\circ d\mathbf{w}(t)=\frac{\phi_f^d(t+dt)+\phi_f^d(t)}{2}[\mathbf{w}(t+dt)-\mathbf{w}(t)]. \tag{B10}$$

Since $\phi_f^d(t)$ is independent of the future stochastic processes $\mathbf{w}(t+dt)-\mathbf{w}(t)$, the Ito product has a notable property

$$\langle\!\langle\phi_f^d(t)\cdot d\mathbf{w}(t)\rangle\!\rangle=\langle\!\langle\phi_f^d(t)\rangle\!\rangle\langle\!\langle d\mathbf{w}(t)\rangle\!\rangle=0, \tag{B11}$$

where we used (B4) for the second equality. This property often simplifies our calculations. From the definitions (B9) and (B10), we have the formula connecting the Stratonovich product with the Ito product in the form

$$\phi_f^d(t)\circ d\mathbf{w}(t)=\phi_f^d(t)\cdot d\mathbf{w}(t)+\frac{1}{2}d\phi_f^d(t)d\mathbf{w}(t). \tag{B12}$$

As stated in subsection II D, we regard the stochastic product appeared in (B1) as that of the Stratonovich type.

Applying the formula (B12) to $d\Omega(t)\circ\phi_f^d(t)$ in (B1), and neglecting the terms of order higher than dt, we have the stochastic equation of the Ito type

$$d\phi_f^d(t)=d\Omega(t)\cdot\phi_f^d(t)+\Psi_f(t)dt, \tag{B13}$$

where

$$\begin{aligned} d\Omega(t) &= d\Omega(t)+\frac{1}{2}d\Omega(t)d\Omega(t) \\ &= d\Omega(t)+\nabla^2\frac{k_BT}{\zeta_N}dt \\ &= -\nabla\cdot\left[\left(\hat\kappa(t)-\frac{K_N}{\zeta_N}\right)\mathbf{r}-\frac{k_BT}{\zeta_N}\nabla\right]dt-\frac{1}{\zeta_N}\nabla\cdot d\mathbf{w}(t). \end{aligned} \tag{B14}$$

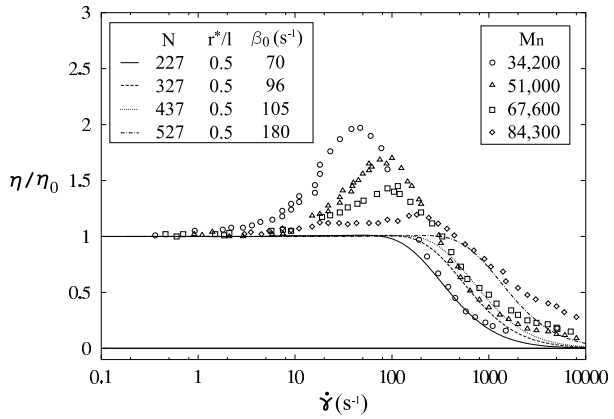

FIG. 10: The steady shear viscosity plotted against the shear rate (TE limit). The lines represent theoretical (TE limit) results obtained for each M_n listed in Table I with $r^*/l=0.5$. The dots represent the experimental results observed for $T=$ 298K and $c=1$wt%.[1] The zero-shear viscosity η_0 is 3.0Poise for $M_n=34,200$, 0.94Poise for $M_n=51,000$, 0.53Poise for $M_n=67,600$ and 0.26Poise for $M_n=84,300$.[1]

Taking the random average of the stochastic equation (B13), we obtain the Fokker-Planck equation

$$\begin{aligned} d\phi^d(t) = &-\nabla\cdot\left(\left[\left(\hat\kappa(t)-\frac{K_N}{\zeta_N}\right)\mathbf{r}-\frac{k_BT}{\zeta_N}\nabla\right]\phi^d(t)\right)dt \\ &+\Psi(t)dt, \end{aligned} \tag{B15}$$

where $\phi^i(t)=\langle\!\langle\phi_f^i(t)\rangle\!\rangle$ as defined in subsection II D. In order to obtain (B15) from (B13), we used the property of the Ito product (B11).

As for the equations (4.1) and (4.3), since they do not contain the stochastic process $\mathbf{R}(t)$ explicitly, we can obtain (4.4) and (4.6) in a straightforward way by taking the random average of (4.1) and (4.3), respectively.

APPENDIX C: SHEAR VISCOSITY (WITHOUT LOOPS)

1. TE Limit

Here, we compare the steady shear viscosity observed by Jenkins *et al.*[1] with that given by the TE limit (Figure 10) for each molecular weight listed in Table I. As mentioned in subsection IV C, the TE limit is attained by adopting small r^* and putting $v_0=0$ in equation (4.63). Since p is given through (5.1) or (5.2), the number of adjustable parameters is two, i.e., β_0 and r^*.

We adopt $r^*=0.5l$ here, although the value is not so small enough being good for the Gaussian model or the Hookean force assumption.[43] With this r^*, the value of β_0 is determined by adjusting the theoretical curve to experimental data *at the shear-thinning region* (the abscissa is scaled by β_0 for given N). For example, the

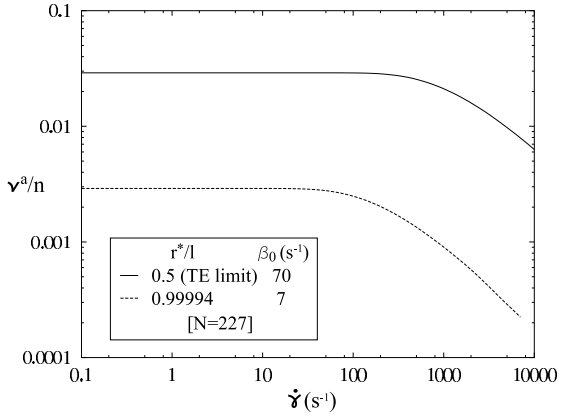

FIG. 11: The number of active chains plotted against the shear rate for $N=227$. The solid line stands for the number of active chains within the TE limit which corresponds to the solid line in Figure 10. The dashed line represents the number of active chains corresponding to the solid line in Figure 13.

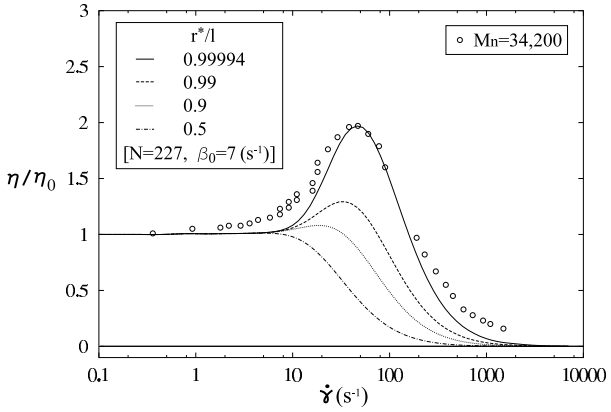

FIG. 12: The steady shear viscosity plotted against the shear rate (without loops). The lines represent theoretical results ($v_0=0$) obtained for $r^*/l=0.5$, 0.9, 0.99 and 0.99994 with fixed $N=227$ and $\beta_0=7\text{s}^{-1}$. The dots represent the experimental results observed for $M_n=34,200$, $\eta_0=3.0$Poise, $T=298$K and $c=1$wt%.[1]

adjusted value of β_0 is 70s^{-1} for $N=227$ ($M_n=34,200$) giving us the lifetime $1/\beta_0\simeq 0.01$s of active chains. It is much smaller than the observed relaxation time of HEUR aqueous solutions having the order of 0.1s.[1,2] The values of β_0 for other N are given inside the box in Figure 10.

We see from these figures that the shear viscosity decreases monotonically as the shear rate increases, i.e., the shear-thickening behavior does not appear within the TE limit. With increasing the shear rate, the number of *longer* active chains increases. The chains which exceed r^* dissociate from the junction and become dangling chains. This causes the decrease in the number of active chains (see the solid line in Figure 11.) leading to the thinning in the shear viscosity. Since r^* is not close to l within the TE limit, the tension of the active chain with end-to-end length r^* is not so strong. Therefore, they can not generate the enhancement of the viscosity. That is the reason why the viscosity rise does not occur in the TE limit.

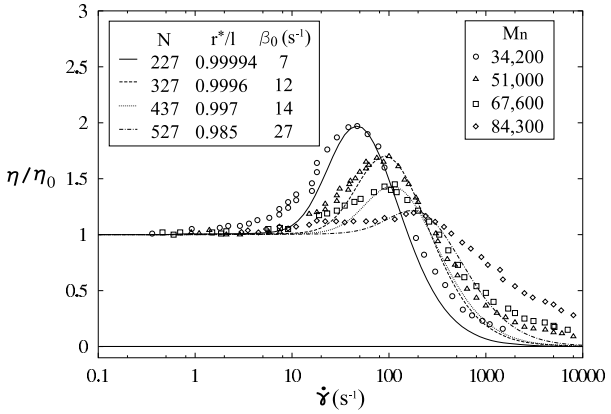

FIG. 13: The steady shear viscosity plotted against the shear rate (without loops.) The lines represent theoretical results ($v_0=0$) obtained for each M_n listed in Table I. The dots represent the experimental results observed for $T=298$K and $c=1$wt%.[1] The zero-shear viscosity η_0 is 3.0 for $M_n=34,200$, 0.94 for $M_n=51,000$, 0.53 for $M_n=67,600$ and 0.26 for $M_n=84,300$.[1]

2. Effects of High-Extension of Active Chains

Let us now see the influence of the stretched active chains on the viscosity. To this end, we consider the case where loops are absent ($v_0=0$) in the wake of the preceding subsection.

The r^* dependence of the steady shear viscosity is shown in Figure 12 for $N=227$ ($M_n=34,200$) and $\beta_0=7\text{s}^{-1}$. From Figure 12, we see that a peak starts to appear when $r^*\gtrsim 0.5l$, and the height of the peak becomes higher with increasing r^*. When $r^*=0.99994l$, it coincides with the experimentally observed one. Note that the appeared peak is narrower than observed one. The value $\beta_0=7\text{s}^{-1}$ is determined so that the position of the peak coincides with observed one. The obtained $1/\beta_0=0.14\text{s}^{-1}$ has the same order as observed relaxation time of HEUR aqueous solutions.[1,2]

Figure 13 shows the theoretically obtained steady shear viscosity with optimal values of r^* and β_0 (given inside the box in the figure) for each molecular weight listed in Table I, compared with experiments. We see from these figures, in common, that 1) the cutoff length r^* is too close to the contour length l, and 2) the peak is too sharp.

The number of active chains for $N=227$ is shown in Figure 11 (the dashed line). As one can see, it monotonically decreases with increasing the shear rate, the reason of which is the same as in the case of $r^*=0.5l$ (i.e., TE

limit). In order to enhance the viscosity against the decreasing number of active chains, we are forced to choose r^* very close to l, since $r^* \lesssim l$ causes the strong force between ends of active chains. That is why r^* so near to l is required to fit the experimental data. The above problems 1) and 2) is resolved by taking account of the open process of loops.

---

[1] Jenkins, R. D.; Silebi, C. A.; El-Aasser, M. S. *ACS Symp. Ser.* **1991**, 462, 222-233.

[2] Annable, T.; Buscall, R.; Ettelaie, R.; Whittlestone, D. *J. Rheol.* **1993**, 37, 695-726.

[3] Yekta, A.; Duhamel, J.; Adiwidjaja, H.; Brochard, P.; Winnik, M.A. *Langmuir* **1993**, 9, 881-883.

[4] Yekta, A.; Xu, B.; Duhamel, J.; Adiwidjaja, H.; Winnik, M.A. *Macromolecules* **1995**, 28, 956-966.

[5] Xu, B.; Yekta, A.; Li, L.; Masoumi, Z.; Winnik, M. A. *Colloids Surf. A* **1996**, 112, 239-250.

[6] Tam, K. C.; Jenkins, R. D.; Winnik, M. A.; Bassett, D. R. *Macromolecules* **1998**, 31, 4149-4159.

[7] Le Meins, J. F.; Tassin, J. F. *Macromolecules* **2001**, 34, 2641-2647.

[8] Maus, C.; Fayt, R.; Jérôme, R.; Teyssié Ph. *Polymer* **1995**, 36, 2083-2088.

[9] Bhargava, S.; Cooper, S. L. *Macromolecules* **1998**, 31, 508-514.

[10] Indei, T. Ph.D. Thesis; University of Tsukuba: Japan, January 2002.

[11] Vrahopoulou, E. P.; McHugh, A. J. *J. Rheol.* **1987**, 31, 371-384.

[12] Marrucci, G.; Bhargava, S.; Cooper, S. L. *Macromolecules* **1993**, 26, 6483-6488.

[13] Séréro, Y.; Jacobsen, V.; Berret, J.-F. *Macromolecules* **2000**, 33, 1841-1847.

[14] Green, M. S.; Tobolsky, A. V. *J. Chem. Phys.* **1946**, 14, 80-92.

[15] Lodge, A. S. *Trans. Faraday Soc.* **1956**, 52, 120-130.

[16] Yamamoto, M. *J. Phys. Soc. Jpn.* **1956**, 11, 413-421; **1957**, 12, 1148-1158; **1958**, 13, 1200-1211.

[17] Tanaka, F.; Edwards, S. F. *Macromolecules* **1992**, 25, 1516-1523.

[18] Tanaka, F.; Edwards, S. F. *J. Non-Newtonian Fluid Mech.* **1992**, 43, 247-271; 273-288; 289-309.

[19] Wang, S. Q. *Macromolecules* **1992**, 25, 7003-7010.

[20] Vaccarro, A.; Marrucci, G. *J. Non-Newtonian Fluid Mech.* **2000**, 92, 261-273.

[21] Warner, H. R. *Ind. Eng. Chem. Fundamentals* **1972**, 11, 379-387.

[22] de Gennes, P. G. *J. Chem. Phys.* **1971**, 55, 572-579.

[23] Doi, M.; Edwards, S. F. *J. C. S. Faraday Trans. 2* **1978**, 74, 1789-1801; 1802-1817; 1818-1832; **1979**, 75, 38-54.

[24] Stratonovich, R. *J. SIAM Control* **1966**, 4, 362-371.

[25] Kubo, R. *J. Math. Phys.* **1963**, 4, 174-183.

[26] See, for instance, Doi, M./translated by See, H. *Introduction to Polymer Physics*; Oxford University Press: Oxford, U.K., 1996; Chapter 4.

[27] Jenkins, R.D.; Bassett, D.R.; Silebi, C.A.; El-Aasser, M.S. *J. Appl. Polym. Sci.* **1995**, 58, 209-230.

[28] Indei, T. Master Thesis; University of Tsukuba: Japan, June 1999.

[29] See, for instance, de Gennes, P.G. *Scaling Cocepts in Polymer Physics*; Cornell University Press: Ithaca, 1979; Chapter 1.

[30] Witten, T. A.; Cohen, M. H. *Macromolecules* **1985**, 18, 1915-1918.

[31] Ballard, M. J.; Buscall, R.; Waite, F. A. *Polymer* **1988**, 29, 1287-1293.

[32] See, for instance, Namiki, M. *Stochastic Quantization*; Springer-Verlag: Berlin, 1992; Appendix B.

[33] Ito, K. *Proc. Imp. Acad. Tokyo* **1944**, 20, 519-524.

[34] The latter effect has been taken into account through the rate equation $\mu\nu^f = q\nu^{d}$[19] within the model, where ν^f (ν^d) is the number of free (dangling) chains in unit volume, and μ (q) is the transition rate from a free (dangling) to a dangling (free) chain.

[35] The stochastic Liouville equation is the one for the probability distribution function in phase space where a point in the space represents a state of the system. Since the mathematical structure of (4.2) is the same as that of the stochastic Liouville equation, we will call (4.2) the stochastic Liouville equation. In the same sense, we will call (4.5) the Fokker-Planck equation.

[36] (4.10) is the equation used by Vaccaro and Marrucci[20] in the long time limit.

[37] This limit was adopted in some literatures.[17,19]

[38] Note that we can use (2.12) instead of (2.14) when τ is 0.

[39] In the literature,[27] four distinct values of $\sqrt{\langle r^2\rangle_0}$ at 30°C are reported for each molecular weight, which were obtained using four different theoretical relations connecting $\sqrt{\langle r^2\rangle_0}$ and the intrinsic viscosity $[\eta]$. The values of $\sqrt{\langle r^2\rangle_0}$ listed in Table I are mean values of these data. Although the steady shear viscosity we are going to analyze is observed at 25°C, since $[\eta]$, and therefore $\sqrt{\langle r^2\rangle_0}$, do not change their values so much within the temperature range $25 \sim 30$°C (see Figures 7,8 and 9 in the literature[27]), we can use $\sqrt{\langle r^2\rangle_0}$ at 30°C to analyze the steady shear viscosity at 25°C.

[40] At equilibrium state, the conformation of a dangling chain is regarded as the Gaussian.

[41] Their discussions are not based on the transient network theory.

[42] That is, the shear-induced transfer of loops to active chains via dangling chains, by means of *frictional force due to solvent*.

[43] This reason is as follows. For smaller r^*, the viscosity starts to decrease at lower shear rates, since the lifetime of an active chain is shorter effectively in this case. It means that, for smaller r^*, we have to adopt larger β_0 (smaller $1/\beta_0$) so that the theoretical results fit to experimental data at the shear-thinning region. Therefore, in order to get larger $1/\beta_0$ close to the observed relaxation time, we have to choose larger r^*. Although the value $r^* = 0.5l$ generates stronger force compared with Hookean force, it does not cause viscosity rising. This value seems to be the critical one for generating the shear-thickening behavior (see Figure 12).